Zebrafish *fgf24* functions with *fgf8* to promote posterior mesodermal development

Bruce W. Draper[1,*,†], David W. Stock[2] and Charles B. Kimmel[1]

[1]Institute of Neuroscience, University of Oregon, Eugene, OR 97403, USA
[2]Department of Environmental, Population and Organismic Biology, University of Colorado, Boulder, CO 80309, USA

*Present address: Basic Sciences Division, Fred Hutchinson Cancer Research Center, Seattle, WA 98109, USA
†Author for correspondence (e-mail: draper@fred.fhcrc.org)

Accepted 12 June 2003

Development 130, 4639-4654

doi:10.1242/dev.00671

Summary

Fibroblast growth factor (Fgf) signaling plays an important role during development of posterior mesoderm in vertebrate embryos. Blocking Fgf signaling by expressing a dominant-negative Fgf receptor inhibits posterior mesoderm development. In mice, *Fgf8* appears to be the principal ligand required for mesodermal development, as mouse *Fgf8* mutants do not form mesoderm. In zebrafish, Fgf8 is encoded by the *acerebellar* locus, and, similar to its mouse otholog, is expressed in early mesodermal precursors during gastrulation. However, zebrafish *fgf8* mutants have only mild defects in posterior mesodermal development, suggesting that it is not the only Fgf ligand involved in the development of this tissue. We report here the identification of an *fgf8*-related gene in zebrafish, *fgf24*, that is co-expressed with *fgf8* in mesodermal precursors during gastrulation. Using morpholino-based gene inactivation, we have analyzed the function of *fgf24* during development. We found that inhibiting *fgf24* function alone has no affect on the formation of posterior mesoderm. Conversely, inhibiting *fgf24* function in embryos mutant for *fgf8* blocks the formation of most posterior mesoderm. Thus, *fgf8* and *fgf24* are together required to promote posterior mesodermal development. We provide both phenotypic and genetic evidence that these Fgf signaling components interact with *no tail* and *spadetail*, two zebrafish T-box transcription factors that are required for the development of all posterior mesoderm. Last, we show that *fgf24* is expressed in early fin bud mesenchyme and that inhibiting *fgf24* function results in viable fish that lack pectoral fins.

Supplementary data available online

Key words: Fibroblast growth factor, *fgf24*, *fgf8*, *acerebellar*, *no tail*, *spadetail*, Mesoderm, Posterior development, Limb development, Zebrafish

Introduction

In vertebrate embryos, the posterior body and tail develop in an anterior to posterior progression by the coordinated growth and morphogenesis of precursor cells located in the tail bud (Kanki and Ho, 1997; Davis and Kirschner, 2000). Studies in several organisms have established that the Fgf signaling pathway plays an essential role during the development of the posterior body, perhaps by maintaining a population of posterior precursors cells during embryogenesis. Inhibiting Fgf signaling in *Xenopus* or zebrafish embryos by overexpressing a dominant-negative Fgf receptor (dnFgfr) blocks the formation of posterior body structures, including all posterior mesoderm (Amaya et al., 1991; Amaya et al., 1993; Griffin et al., 1995). Similarly, mouse embryos mutant for the Fgf receptor 1 (*Fgfr1*), one of four known vertebrate Fgf receptors, produce limited amounts of posterior mesoderm (Yamaguchi et al., 1994; Deng et al., 1994). *Fgfr1* is cell autonomously required for posterior mesodermal development, as *Fgfr1* mutant cells transplanted into wild-type host embryos do not contribute to this tissue, and instead adopt neuronal fates (Ciruna et al., 1997; Ciruna and Rossant, 2001). Thus, the Fgf signaling pathway appears to play a conserved role during development of posterior mesoderm in vertebrates.

To date, 23 Fgf ligands (Fgf1-23) have been described in tetrapods (reviewed by Ornitz and Itoh, 2001) and several of these ligands are known to be expressed in early mesodermal progenitors in mice, including *Fgf3* (Wilkinson et al., 1988), *Fgf4* (Niswander and Martin, 1992; Drucker and Goldfarb, 1993), *Fgf5* (Haub and Goldfarb, 1991; Hébert et al., 1991) and *Fgf8* (Heikinheimo et al., 1994; Ohuchi et al., 1994; Crossley and Martin, 1995). Mutational analyses in mice, however, suggest that not all of these ligands are required for the development of mesoderm. For example, embryos mutant for *Fgf3* and *Fgf5* have only slight (*Fgf3*) (Mansour et al., 1993) or no (*Fgf5*) (Hébert et al., 1994) defects in posterior development. Conversely, *Fgf8* mutant embryos do not form posterior mesoderm, indicating that *Fgf8* activity can account for the majority of Fgf signaling required for posterior development in mice. A role for *Fgf4* in posterior mesodermal development in mice has yet to be established, as *Fgf4* mutants die prior to mesoderm formation (Feldman et al., 1995).

In addition to Fgf signaling, T-box genes, which function as transcriptional regulators, are also required for formation of the posterior body during vertebrate embryogenesis. The founding member of the T-box gene family, mouse *T* or *Brachyury* is expressed early in mesodermal precursors and then in the developing notochord (Herrmann et al., 1990). *T* is required for the development of these tissues, as *T* mutant embryos fail to form a notochord and lack posterior body structures (reviewed by Smith, 1999; Papaioannou, 2001). The role of *T* in mesodermal development appears to be evolutionarily conserved in vertebrates, as *T* orthologs in several organisms have been shown to have similar expression patterns and functions. For example, *T* orthologs in *Xenopus* and zebrafish, called *Xbra* and *no tail* (*ntl*), respectively are expressed in mesodermal precursors and in the developing notochord (Smith, et al., 1991; Schulte-Merker et al., 1992), and are required (Halpern et al., 1993; Conlon et al., 1996) and sufficient (Cunliff and Smith, 1992; O'Reilly et al., 1995) for notochord and posterior mesodermal development.

The T-box gene *VegT/spt* has also been implicated in mesodermal specification in vertebrate embryos. *VegT* in *Xenopus* is expressed in mesodermal precursors and in developing posterior paraxial mesoderm, and is also expressed maternally (Horb and Thomsen, 1997; Lustig et al., 1996; Stennard et al., 1996; Zhang and King, 1996). Inhibition of maternal *VegT* function results in embryos that fail to form both mesoderm and endoderm, showing that *VegT* has an early role in germ layer formation (Zang et al., 1998). The function of zygotically expressed *VegT* has not been determined. In zebrafish, *spadetail* (*spt*; *tbx16* – Zebrafish Information Network) is an ortholog of *VegT* and is similarly expressed in mesodermal precursors and in developing paraxial mesoderm. In contrast to *VegT*, however, *spt* is not expressed maternally (Griffin et al., 1998). *spt* mutant embryos lack paraxial mesoderm in the trunk, but not in the tail, and form a relatively normal notochord (Kimmel et al., 1989; Amacher et al., 2002). Thus, *spt* mutants have a phenotype that is nearly reciprocal to that of *ntl* mutants. Although both *spt* and *ntl* mutants form lateral and ventral mesodermal cell types, *spt;ntl* double mutant embryos fail to form all posterior mesoderm (Amacher et al., 2002). These results suggest that *spt* and *ntl* have distinct roles in promoting the development of specific mesodermal subtypes, as well as a presumed earlier, and redundant role in the specification of all posterior mesodermal precursors.

A link between Fgf signaling and T-box gene function in posterior mesodermal development was revealed when it was shown that T-box gene expression in mesodermal precursors is dependent on Fgf signaling. In *Xenopus* and zebrafish, expression of *Xbra*/*ntl* is inhibited when Fgf signaling is blocked (Amaya et al., 1991; Isaacs et al., 1994; Schulte-Merker and Smith, 1995; Griffin et al., 1995) and ectopic activation of the Fgf signaling pathway leads to ectopic *Xbra/ntl* expression (Isaacs et al., 1994; Schulte-Merker and Smith, 1995; Griffin et al., 1995). These and other results have led to the model that Fgf signaling and T-box genes form an auto-regulatory feedback loop during early mesodermal development, where the function of one component is necessary for the continued expression of the other. These interactions are thought to promote posterior development by maintaining and regulating the growth and morphogenesis of mesodermal precursors in the posterior region of the embryo (reviewed by Isaacs, 1997).

In zebrafish, inhibiting Fgf signaling leads to a phenotype that is strikingly similar to that of *spt;ntl* double mutant embryos (Griffin et al., 1995; Amacher et al., 2002). Because expression of both *spt* and *ntl* in mesodermal precursors is Fgf dependent (Griffin et al., 1995; Griffin et al., 1998), it is possible to explain the mesodermal defects associated with blocking Fgf signaling as a loss of *spt* and *ntl* function. Although *spt* and *ntl* are key regulators of posterior development in zebrafish, little is known about which Fgf signaling components are required to maintain their expression.

The zebrafish *fgf8* gene is expressed in mesodermal precursors and is therefore a candidate Fgf ligand for regulating posterior development. A mutation in *fgf8* (or *acerebellar*) (Reifers et al., 1998), has been identified, but unlike embryos injected with a dnFgfr (Griffin et al., 1995), *fgf8* mutants (Reifers et al., 1998), or embryos in which *fgf8* function has been inhibited with morpholino oligonucleotides (Araki and Brand, 2001; Draper et al., 2001) have relatively mild defects in posterior development. A hypothesis that we explore here is that additional Fgf ligands function together with Fgf8 during development of the posterior body in zebrafish.

We have identified and characterized a second Fgf ligand-encoding gene in zebrafish that is expressed in mesodermal precursors. This ligand is a new, but distinct, member of the *fgf8/17/18* subclass of Fgf ligands, for which there is no ortholog among the 23 known Fgfs in tetrapods. We therefore designate this gene *fgf24*. We show that *fgf24* is expressed in a domain that overlaps extensively with that of *fgf8*, *ntl* and *spt* in mesodermal precursors during gastrulation, and that *fgf8* and *fgf24* are together required for the formation of most posterior mesoderm. Furthermore, we present both gene expression and genetic data showing that interactions between the Fgf signaling pathway and the *ntl* and *spt* T-box genes are essential for posterior mesoderm development in zebrafish. Last, we show that *fgf24* is also required for initiation of the pectoral fin bud, a role that appears similar to that of *Fgf10* in mice (reviewed by Martin, 1998).

Materials and methods

Isolation and characterization of *fgf18* and *fgf24* cDNAs

Degenerate primers for RT-PCR of *fgf8*-related genes (5′-GCCG<u>GGATCC</u>ACNAGYGGNAARCAYGTNCA-3′ and 5′-GCCG<u>GAATTC</u>GGNARNCKYTTCATRAARTG-3′, where the underlined sequences represent restriction sites added for cloning) were designed from an alignment of tetrapod *Fgf8* sequences. PCR was carried out on cDNA produced from mRNA isolated from 5-day-old larvae. PCR products were cloned into pBluescript II SK$^+$ (Stratagene, La Jolla, CA) and 34 independent clones were sequenced. Of these, seven were identified as *fgf8*, two as *fgf17*, seventeen as *fgf18* and eight as *fgf24*, based on phylogenetic analyses of the 105-106 encoded amino acids. An *fgf24* cDNA was isolated by using one of the cloned RT-PCR fragments as a probe to screen a gastrula-stage cDNA library (a gift from T. Lepage and D. Kimelman). Additional *fgf18* cDNA sequence was isolated by 3′ and 5′ RACE using the First Choice RLM-RACE kit (Ambion, Austin, TX) following the manufacturer's instructions. The *fgf24* gene structure was determined by partially sequencing a PAC clone containing the *fgf24* gene. This clone was identified by screening a PAC library (Amemiya and Zon, 1999) by PCR with the gene specific primers 5′-CAGGAGTG-CGTCTTCGTGGAG-3′ and 5′-GTGCCCTTCGTGTCCTTTTCG-3′ (231 bp fragment). Temporal expression profiles were determined by RT-PCR, as previously described (Draper et al., 2001) using the following primers (5′ primer/3′ primer): *fgf8*, CACATTTGGGAG-TCGAGTTCG/GTGCTCTGCGATTTGGTGTCC (288 bp fragment);

fgf24, GCAAGAAGATTAACGCCAATGG/TTTAGGTCGACCCTT-TCG (272 bp fragment); *fgf18*, GACGACGGAGATAAATATGCC/CGTACCATCCTGTGTAGCGC (221 bp fragment); and *odc*, ACAC-TATGACGGCTTGCACCG/CCCACTGACTGCACGATCTGG (309 bp fragment). GenBank Accession Numbers for the cDNA sequences are: *fgf18*, AY243514; *fgf24*, AY204859.

Sequence alignment and phylogenetic analysis

Phylogenetic relatedness of *fgf24* and *fgf18* were determined by aligning sequences with the ClustalX program, and constructing trees from the alignments using the neighbor-joining method. Prior to alignment, we used the Signal IP program (Nielsen et al., 1997) to identify the most probable cleavage site of the signal peptide that comprises the N-terminal 25-30 amino acids of the proteins. The tree was then constructed using an alignment that contained only those sequences that were predicted to be present in the mature Fgf proteins. As an outgroup, the distantly related zebrafish Fgf10 protein sequence was used.

Mapping

The positions of *fgf18*, *fgf24* and the EST fi43f07 (GenBank Accession Number AW174476; M. Clark and S. Johnson, WUZGR; http://zfish.wustl.edu) in the zebrafish genome were determined by mapping on the Goodfellow T51 radiation hybrid (RH) panel (Kwok et al., 1998) (Research Genomics) using the following primers pairs (5′ primer/3′ primer): *fgf18*, CCGGGACTCAAACCAGCGACC/GTCCTGCTGGTTGGGAAGCG (411 bp fragment); *fgf24*, same primers as those used for PAC isolation (see above); fi43f07, GTTCACCGACGGGTTTCCATTTTCA/TCCTGCATCTTTAGCCC-GCGTTTAC (199 bp fragment). Following PCR, fragments were separated by electrophoresis and scored as described by Geisler et al. (Geisler et al., 1999). The RH data was converted to a map position using the Instant Mapping program (http://134.174.23.167/zonrhmapper/instantMapping.htm).

Fish stocks and maintenance

Adult zebrafish stocks and embryos were maintained at 28.5°C as described previously (Westerfield, 1995). Embryos were produced by natural matings of the appropriate adult fish. Embryos were collected and sorted at early cleavage stages and maintained in embryo medium (Westerfield et al., 1995) at 28.5°C until the desired developmental stages according to Kimmel et al. (Kimmel et al., 1995). The following alleles were used for this study: *fgf8/acerebellar*^{ti282}, *spt*^{b104} and *ntl*^{b195}. The *spt*^{b104} (Griffin et al., 1998) and *ntl*^{b195} (Schulte-Merker et al., 1994) alleles are null, while the *fgf8*^{ti282} allele is probably a hypomorph (Draper et al., 2001). *spt* maps to LG8 (S. L. Amacher, unpublished), *Fgf8* maps to LG13 (Woods et al., 2000) and *ntl* maps to LG19 (Postlethwait et al., 1998).

Fish doubly heterozygous for *spt*^{b104} and *fgf8*^{ti282}, or for *fgf8*^{ti282} and *ntl*^{b195} were generated by crossing single heterozygotes of the appropriate genotype to produce F_1 offspring. The genotypes of adult F_1 fish were scored by crossing to tester fish of known genotype. Homozygous double mutant embryos were then produced by crossing doubly heterozygous fish. Embryos from such crosses were sorted into phenotypic classes based on morphology at 24 hpf using a dissecting microscope. For two unlinked mutations segregating in a Mendelian fashion, four phenotypic classes should be obtained in a ratio of 9:3:3:1 (wild type:mut1$^{-/-}$:mut2$^{-/-}$:mut1$^{-/-}$:mut2$^{-/-}$). In crosses between *spt*$^{+/-}$;*fgf8*$^{+/-}$ fish, the following phenotypic classes were found in the ratios of 9.07:3.08:2.91:0.94 (wild type:*spt*$^{-}$:*fgf8*$^{-}$:*spt*$^{-}$;*fgf8*$^{-}$, n=1,076, x^2=0.612, P>0.80). In crosses between *fgf8*$^{+/-}$;*ntl*$^{+/-}$ fish, the following phenotypic classes were obtained in the ratios of 8.83:3.13:2.94:1.10 (wild type:*fgf8*$^{-}$:*ntl*$^{-}$:*fgf8*$^{-}$;*ntl*$^{-}$, n=609, x^2=0.76, P>0.80). In crosses between *fgf8*$^{+/-}$;*ntl*$^{+/-}$ double heterozygotes and *fgf8*$^{+/-}$ single heterozygous fish, the following phenotypic classes were obtained in the ratios of 6.03:0.94:1.03 (wild type:*fgf8*$^{-}$:*fgf8*$^{-}$ short tail, n=382, x^2=0.196, P>0.90).

Tissue labeling

Riboprobes for in situ hybridization were synthesized using the MaxiScript kit according to the manufacturer's instructions (Ambion, Austin, TX). With the exception of *fgf24* (this paper), the probes used have been described previously as follows: *pax2.1* (Krauss et al., 1991), *krx20* (*egr2* – Zebrafish Information Network) (Oxtoby and Jowett, 1993), *myod* (Weinberg et al., 1996), *ntl* (Schulte-Merker et al., 1992), *spt* (Griffin et al., 1998), *fgf8* (Fürthauer et al., 1997; Reifers et al., 1998) and *shh* (Krauss et al., 1993). The *fgf24* in situ probe was transcribed from the full length cDNA. Immunohistochemical staining with anti-Ntl (Schulte-Merker et al., 1992) and anti-Spt (Amacher et al., 2002) were preformed as detailed by Amacher et al. (Amacher et al., 2002). For in situ hybridization experiments using embryos older than 24 hpf, melanogenesis was inhibited by raising embryos in embryo medium containing 0.003% PTU (1-phenyl 2-thiourea) (Westerfield, 1995). For sectioning, embryos were embedded in epon and 7.5 μm sections were cut.

Morpholino injection and RNase protection assays

The splice-site targeted morpholino oligonucleotide (MO) *fgf24*-E3I3 was obtained from GeneTools (Corvalis, OR) and has the following sequence: 5′-AGGAGACTCCCGTACCGTACTTGCC-3′. MO injections were performed as previously described (Draper et al., 2001). RT-PCR analysis shown in Fig. 3 was performed essentially as described above, but using the *fgf24* specific PCR primer pair (5′ primer/3′ primer): CGGCAAACGCTGGAAACAGG/GTCTCTGTC-TCCACCACAAGC (wild-type fragment 300 bp). RNase protection assays were performed using the RPA III kit (Ambion, Austin, TX) as previously described (Draper et al., 2001). A template for making antisense *fgf24* probe was generated by amplifying a fragment of the *fgf24* cDNA using the primer pair ATGTCTGTTCTGCCGTCAAGG/GTCTCTGTCTCCACCACAAGC, and cloning into the pCRII-TOPO TA vector (Invitrogen, Carlsbad, CA).

Skeletal staining

One-month-old fish were cleared and stained for bone (with Alizarin Red) and cartilage (with Alcian Green) as described by Grandel and Schulte-Merker (Grandel and Schulte-Merker, 1998).

Results

Identification and molecular characterization of zebrafish *fgf18* and *fgf24*

In zebrafish, the mesodermal and endodermal germ layers form from precursor cells located at the margin of the early gastrula embryo (Kimmel et al., 1990). During gastrulation, these cells involute at the margin to form the hypoblast layer under the overlying epiblast layer, which contains ectodermal precursors (Warga and Kimmel, 1990; Warga and Nusslein-Volhard, 1999). *fgf8* has previously been shown to be expressed in mesendodermal precursor cells during gastrulation in zebrafish (Fürthauer et al., 1997; Reifers et al., 1998). We sought to identify additional Fgf ligands that are expressed in mesendodermal precursors during gastrulation and focused on identifying *fgf8*-related genes. Using degenerate oligonucleotide primers that were designed to amplify genes closely related to *fgf8*, we isolated four distinct cDNA fragments. In addition to fragments corresponding to *fgf8* (Fürthauer et al., 1997; Reifers et al., 1998) and *fgf17* (Reifers et al., 2000), we identified fragments from two genes whose sequence appeared most closely related to tetrapod *Fgf18* (Ohbayashi et al., 1998; Hu et al., 1999).

To further characterize these two genes, we identified and sequenced cDNAs, and used their conceptually translated protein sequences to construct a phylogenetic tree (Fig. 1A,B). Sequence comparison to the 22 known human FGF ligands confirmed that these two genes are members of the *FGF8/17/18* subfamily (henceforth referred to as 'Fgf8 subfamily') (reviewed by Ornitz and Itoh, 2001) and are most closely related to *FGF18* (not shown). Of the two zebrafish proteins, one shared 73% amino acid identity with human *FGF18*, while the other shared only 65% identity (Fig. 1A,B). For simplicity, we shall refer to these genes as *fgf18* and *fgf24* respectively. To better determine the relationship of *fgf18* and *fgf24* to known genes, we mapped them using the T51 radiation hybrid panel (Kwok et al., 1998) and found that they both localized to LG14, ~18 cM apart (Fig. 1C). Human *FGF18* has been mapped to chromosome 5q34 (Whitmore et al., 2000), and previous studies have found that LG14 contains regions with conserved synteny to human 5q31-5q35 (Woods et al., 2000). Using these data, together with the map positions of additional zebrafish orthologs of human genes known to map in the 5q31-5q35 interval, we determined that there was significant conserved synteny between regions containing zebrafish *fgf18* and human *FGF18*. For example, the human gene encoding the F-box WD40 protein *FBXWB1*, and its

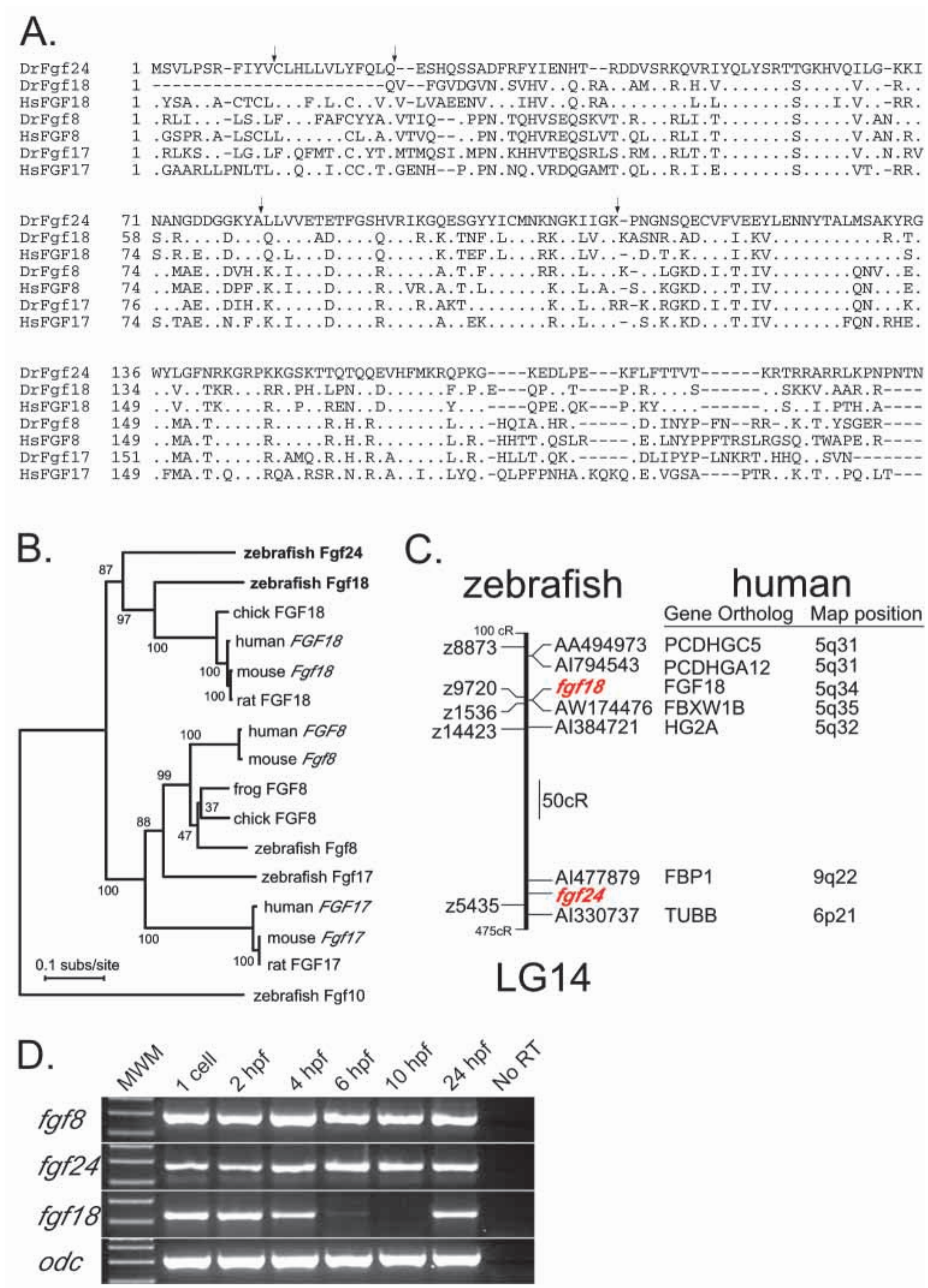

Fig. 1. *fgf24* is a member of the *fgf8/17/18* subfamily and is expressed during gastrulation. (A) Sequence comparison of the predicted amino acid sequences of zebrafish (Dr) Fgf24, Fgf18, Fgf8 and Fgf17, with human (Hs) *FGF18*, *FGF8* and *FGF17*. Periods indicate identical residues; dashes indicate introduced gaps; arrows indicate exon boundaries. Only partial sequence for zebrafish Fgf18 is shown as the 5′ end of the gene has not been identified. (B) Phylogenetic tree comparing the relatedness of zebrafish Fgf18 and Fgf24 with other members of the Fgf8 subfamily. Zebrafish Fgf10 is distantly related to the Fgf8 subfamily, and was included as an outgroup. Numbers indicate bootstrap support for the nodes. (C) *fgf18* and *fgf24* map to LG 14. Map position of *fgf18* and *fgf24,* as determined by screening the T51 radiation hybrid panel is shown relative to representative zmarkers (left) and ESTs (right, listed by GenBank Accession Numbers). The entire linkage group is not shown. Zebrafish genes that are closely linked to zebrafish *fgf18* have human homologs that are closely linked to human *FGF18.* (D) Temporal expression profiles for zebrafish *fgf18* and *fgf24* in comparison with *fgf8* as determined by RT-PCR. The zebrafish *ornithinedecarboxylase* (*odc*) gene was used as an internal control (see Draper et al., 2001). cR, centiRay; MWM, molecular weight marker; hpf, hours post fertilization.

zebrafish ortholog, referred to by its GenBank Accession Number AW174476, are closely linked to *fgf18* (Fig. 1C). By contrast, we found no significant syntenic conservation between the map location of *fgf24* and any region of the human genome. Because Fgf24 protein sequence is as distantly related to Fgf18 orthologs as Fgf8 orthologs are to Fgf17 (Fig. 1B), we propose that Fgf24 defines a new clade in the Fgf8/17/18 subfamily, and for which a tetrapod ortholog has not been described.

We used RT-PCR to compare the temporal expression profiles of *fgf18* and *fgf24* with that of *fgf8*. Similar to *fgf8*, we found that *fgf18* and *fgf24* transcripts could be detected in one-cell stage embryos (Fig. 1D), indicating that these genes are maternally expressed. By contrast, *fgf24*, but not *fgf18*, is also expressed throughout gastrulation (6-10 hpf; Fig. 1D) during the period of mesoderm specification and involution. For the remainder of this study, we focus only on characterizing the expression and function of *fgf24*. The expression and function of *fgf18* will be reported elsewhere (B.W.D. and D.W.S., unpublished).

Analysis of the Fgf24 protein sequence using the SignaIP program (Nielsen et al., 1997) indicates that the C-terminal 30 amino acids encode a probable signal sequence, arguing that *fgf24* is a secreted protein. We determined the intron/exon boundaries of the *fgf24* gene by partial sequencing of the genomic locus and found that they are in positions that are conserved within the Fgf8 subfamily (Xu et al., 1999) (Fig. 1A).

fgf8 and *fgf24* are co-expressed in mesodermal progenitors during gastrulation

We determined the expression pattern of *fgf24* transcripts in gastrula-stage embryos by whole-mount in situ hybridization. We first detected localized *fgf24* transcripts at the beginning of epiboly (6 hpf) in the dorsalmost cells of the blastula margin (not shown) and, soon after, expression extends completely around the margin with no obvious dorsoventral bias (Fig. 2A,B). *fgf24* expression continues in marginal cells throughout gastrulation (Fig. 2C-F) and by the end of gastrulation is localized to the tail bud (Fig. 2G). Thus, *fgf24* has a similar expression pattern to that of *fgf8* in early embryos (Fürthauer et al., 1997; Reifers et al., 1998).

We characterized in more detail the expression of *fgf24* in gastrula-stage embryos by analyzing parasagittal sections of in situ hybridized mid-gastrula stage embryos (8 hpf). We compared the localization of *fgf24* transcripts (Fig. 2H,L) in the paraxial level of the germ ring to that of *fgf8* (Fig. 2I,M), and the mesodermally expressed T-box genes *ntl* (Fig. 2K,O) and *spt* (Fig. 2J,N). Although we found the expression domains of *fgf24* and *fgf8* have significant overlap, they are not identical. Specifically, cells expressing the highest levels of *fgf24* localize to the hypoblast layer of the germ ring (Fig. 2L), and in this regard, expression of *fgf24* is most similar to the expression of *spt* (compare Fig. 2L with 2N) (Griffin et al., 1998). By contrast, cells expressing the highest levels of either *fgf8* or the T-box gene *ntl* localize to the epiblast layer of the germ ring (compare Fig. 2M with 2O) (Fürthauer et al., 1997; Schulte-Merker et al., 1992).

In addition to the germ ring, *fgf8* is also expressed in the presumptive brain beginning at 8 hpf in a domain that spans from the future midhindbrain junction (MHB) posteriorly to rhombomere 4 (Fig. 2I,M) (Reifers et al., 1998; Maves et al., 2002). At this stage of development, *fgf24* is not expressed in the presumptive brain, though weak staining can be seen in dispersed cells within the presumptive spinal cord (Fig. 2E). Thus, the co-expression of *fgf8* and *fgf24* in the germ ring, but

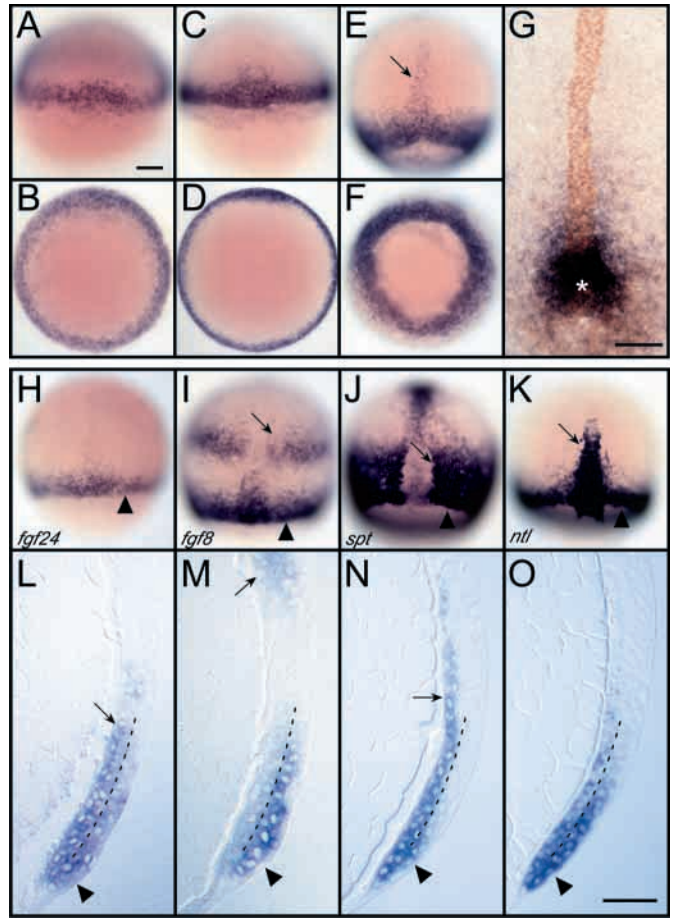

Fig. 2. *fgf24* is expressed in mesodermal precursors during gastrulation in a pattern that overlaps with the expression of *fgf8*, *ntl* and *spt*. Dorsal (A,C,E) and vegetal (B,D,F; dorsal is upwards) views of embryos showing expression of *fgf24* at 4 hpf (A,B), 6 hpf (C,D) and 9 hpf (E,F). In addition to the germ ring, *fgf24* has weak expression in the developing neural ectoderm (arrow in E), as determined by section analysis (not shown). (G) In situ hybridization and immunohistochemistry show the relationship between the expression of *fgf24* (purple) and Ntl (brown) in one-somite-stage embryos. Asterisk indicates the tail bud. The expression pattern of *fgf24* (H,L) is compared with that of *fgf8* (I,M), *spt* (J,N) and *ntl* (K,O) in mid-gastrulation stage embryos (8.5 hpf) by whole-mount in situ hybridization (H-K; dorsal views) and in parasagittal sections (L-O). Arrowheads in H-K indicate approximate position of section though germ ring, and approximate division between the epiblast and hypoblast cell layers in L-O is indicated with a broken line. (L) *fgf24* expression is higher in the hypoblast layer (arrow) relative to the epiblast, similar to the localization of *spt* (N). By contrast, *fgf8* expression is highest in the epiblast (M) similar to the localization of *ntl* (O). In addition to the germ ring staining (arrowheads in H-O), *fgf8* is also expressed in the developing hindbrain (arrow in I,M), *spt* in presomitic mesoderm (arrow in J,N) and *ntl* in the developing notochord (arrow in K). Scale bars: in A, 100 μm for A-K; in O, 50 μm for L-O.

not in the presumptive brain, supports the hypothesis that *fgf24* functions with *fgf8* during posterior mesoderm production and can readily explain why *fgf8* mutant embryos have only mild defects in the development of posterior mesoderm, yet have significant defects in the development of the MHB (Reifers et al., 1998).

fgf24 splice-blocking morpholino oligos knock-down *fgf24* gene function

We directly tested the hypothesis that *fgf24* and *fgf8* function redundantly during the development of posterior mesoderm by knocking down *fgf24* gene function with antisense morpholino oligonucleotides (MOs) (Nasevicicius and Ekker, 2000) targeted to a splice junction site in the *fgf24* pre-mRNA. Splice site-targeted MOs have been shown to alter pre-mRNA splicing when injected into zebrafish embryos, and have the advantage that their efficacy can be quantified by ribonuclease protection (Draper et al., 2001). We obtained a MO targeted to the splice donor site located at the junction of exon 3 and intron 3 (henceforth referred to as *fgf24*-E3I3; Fig. 3A). We first asked if *fgf24*-E3I3 could alter splicing of *fgf24* pre-mRNA using RT-PCR. We injected 5 ng of *fgf24*-E3I3 into one- to four-cell stage embryos and harvested RNA at 24 hpf. Using primers that span exon 3 (Fig. 3A), we found that injection of *fgf24*-E3I3 results in two aberrant splice forms, one of which causes an ~100 bp deletion in the *fgf24* cDNA when compared with cDNA amplified from control embryos (Fig. 3B). We sequenced this RT-PCR product and found that the deletion results from the aberrant use of a cryptic splice donor site located 98 bp upstream of the correct exon 3 splice donor (Fig. 3C). Splicing at this cryptic splice donor shifts the reading frame of *fgf24* mRNA such that only 19 of the 178 amino acids that are predicted to form the secreted Fgf24 protein are encoded. This severely truncated form of Fgf24 is predicted to be non-functional (Fig. 3C).

We next quantified the ability of *fgf24*-E3I3 to reduce the amount of correctly spliced *fgf24* mRNA by ribonuclease protection. We injected *fgf24*-E3I3 into one- to four-cell stage embryos at doses ranging from 1.3-5.0 ng MO/embryo and harvested RNA at 24 hpf. Using a riboprobe that detects correctly spliced message (Fig. 3D) we found that injection of *fgf24*-E3I3 reduced the amount of wild-type *fgf24* mRNA in a dose-dependent manner (Fig. 3E,F). Because injection of 5 ng *fgf24*-E3I3 per embryo reduced the amount of wild-type message to levels that were undetectable in our assay, we chose this amount for all subsequent experiments involving MO-induced knockdown of *fgf24*.

fgf8 and *fgf24* are together required for the production of posterior mesoderm

We asked what effect reducing *fgf24* gene function had on the development of posterior mesoderm by injecting *fgf24*-E3I3 into one- to four-cell stage wild-type embryos to generate *fgf24*^{MO} embryos. We compared the amount of posterior mesoderm produced by injected and control siblings at the 12-somite stage by staining fixed embryos for marker genes that are expressed in restricted domains of posterior mesoderm. We assayed the production of axial mesoderm using anti-Ntl antibodies, which reveal cells in the notochord and tail bud (Schulte-Merker et al., 1992), and paraxial and intermediate mesoderm by in situ hybridization using probes specific for

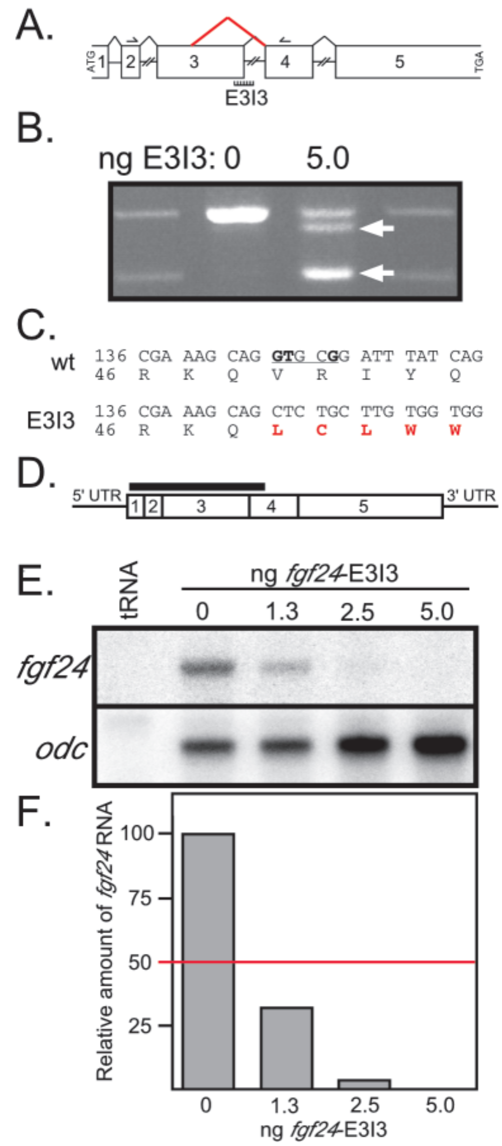

Fig. 3. *fgf24* splice-blocking morpholino oligonucleotides knock down functional *fgf24* mRNA. (A) Genomic structure of the *fgf24* gene. Translation initiation and termination codons are indicated. Exons are shown as boxes and intron sizes are not to scale. Splice donor site targeted by the *fgf24*-E3I3 morpholino oligo is shown. The colored line indicates the major splice variant observed following *fgf24*-E3I3 injection. Primers used for RT-PCR analysis in B are shown as arrows. (B) In addition to wild type (upper band in 5 ng lane), RT-PCR analysis detects two splice variants (arrows). (C) cDNA sequence comparison reveals that the major splice variant (bottom band in B) caused by *fgf24*-E3I3 results from aberrant splicing to an upstream cryptic slice donor site (underlined in wild-type sequence) that is present in exon 3. The sequences derived from exon 4 in the aberrantly spliced form are italicized. Note that use of the cryptic splice site results in a coding frame shift. (D) Position of the *fgf24* antisense RNA probe (bold horizontal line) that was used for RNase protection assays in E is indicated relative to the wild-type *fgf24* mRNA splice junctions (vertical lines). (E) The amount of wild-type *fgf24* mRNA in MO injected and control embryos was determined by RNase protection, using *odc* levels as an internal control. The amount of MO injected per embryo is indicated above lane. (F) Relative levels of wild-type *fgf24* mRNA in E was determined after amounts were normalized using the *odc* control.

myod (Weinberg et al., 1996) and *pax2.1* (Krause et al., 1991), respectively (Fig. 4A). We found that we could not detect differences in marker gene expression when comparing *fgf24^MO^* embryos with wild-type control embryos (compare Fig. 4A with 4B). In addition, we compared the morphology of live *fgf24^MO^* embryos and wild-type embryos at 24 hpf and again could not detect any significant differences (compare Fig. 4E with 4F). Thus, reducing the level of *fgf24* mRNA to undetectable levels in early zebrafish embryos appears to have no detectable effect on the development of posterior mesoderm under our assay conditions.

To test the possibility that lack of *fgf24* function in *fgf24*^{MO} embryos is compensated for by *fgf8* function, we injected *fgf24*-E3I3 into *fgf8* mutant embryos. We will refer to *fgf8*$^{–}$ embryos that have been injected with *fgf24*-E3I3 MO as *fgf8*$^{–}$;*fgf24*^{MO} embryos. At the 12 somite stage, *fgf8*$^{–}$ embryos can be identified by their reduced expression of *pax2.1* in the MHB (Fig. 4C) (Reifers et al., 1998). In addition to the MHB defects, *fgf8* single mutants produce less somitic mesoderm than wild-type embryos (Fig. 4C) (Reifers et al., 1998). In contrast to the effect observed after injection of *fgf24*-E3I3 into wild-type embryos, injection into *fgf8*$^{–}$ embryos resulted in severe defects in posterior mesoderm development. At the 12-somite stage (13 hpf) *fgf8*$^{–}$;*fgf24*^{MO} embryos had a significantly truncated notochord, and produced very few *myod*- and *pax2.1*-expressing cells (Fig. 4D) when compared with control wild-type embryos (Fig. 4A). When live embryos were examined at 24 hpf, *fgf8*$^{–}$;*fgf24*^{MO} embryos lacked the MHB (Fig. 4H), a phenotype that is identical to *fgf8* single mutants (Fig. 4G), and additionally had severely truncated tails relative to wild-type embryos, *fgf8*$^{–}$ or *fgf24*^{MO} embryos (Fig. 4F,G). In this respect, *fgf8*$^{–}$;*fgf24*^{MO} embryos more closely resembled embryos in which Fgf signaling had been inhibited by expression of a dnFgfr (Griffin et al., 1995) or *spt;ntl* double mutant embryos (Amacher et al., 2002).

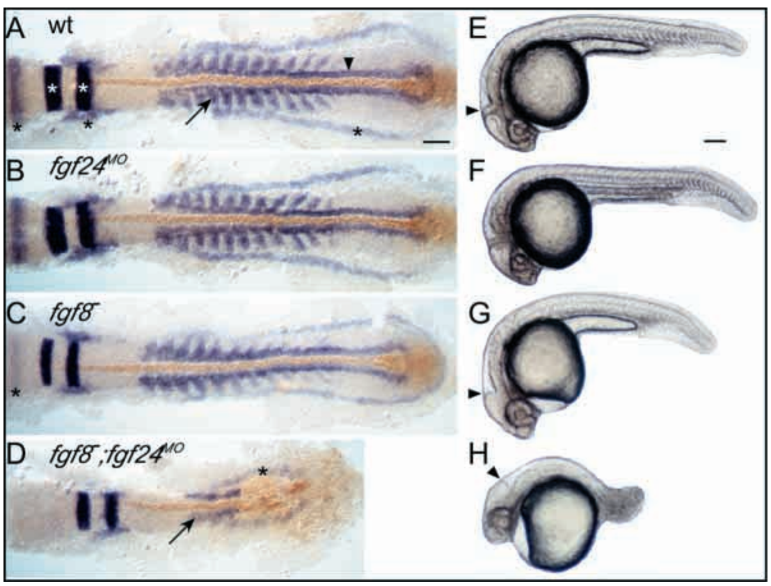

Fig. 4. Functional analysis reveals that *fgf8* and *fgf24* are together required for posterior mesodermal development. In situ hybridization and immunohistochemistry in 10-somite stage wild-type (A), *fgf24*^{MO} embryos (B), *fgf8*$^{–}$ (C) and *fgf8*$^{–}$;*fgf24*^{MO} embryos (D). In A-D, *pax2.1*, *krx20* and *myod* are stained purple, and Ntl protein is stained brown. At this stage in wild-type embryos, *pax2.1* is expressed in the mid-hindbrain boundary (MHB), the otic placode and precursors of the pronephric ducts (black asterisks), *krx20* in rhombomeres 3 and 5 (white asterisks), *myod* in adaxial cells (arrowhead) and a subset of cells in the forming somites (arrow), and Ntl protein in the developing notochord. At this stage, *fgf24*^{MO} embryos (B) are indistinguishable from wild type, while *fgf8* mutants (C) have reduced expression of *pax2.1* in the MHB, and a reduced number of cells expressing *myod* in the forming somites. By contrast, *fgf8*$^{–}$;*fgf24*^{MO} embryos (D) have significantly reduced numbers of *myod*- (arrow), *pax2.1*- (asterisks) and Ntl-expressing cells relative to wild-type, *fgf24*^{MO} and *fgf8*$^{–}$;*fgf24*^{MO} embryos. (E-H) Live wild-type and mutant embryos at 24 hpf. *fgf24*^{MO} embryos (F) are morphologically indistinguishable from wild-type embryos (E), while *fgf8*$^{–}$ embryos (G) have a slightly shorter tail and a prominent MHB defect (arrowhead). *fgf8*$^{–}$;*fgf24*^{MO} embryos (H) have MHB defect (arrowhead), and produce significantly less posterior tissue than either *fgf8* mutant or *fgf24*^{MO} embryos. Scale bars: in A, 50 μm for A-D; in E, 100 μm for E-H.

fgf8 and *fgf24* are together required for maintaining *ntl* and *spt* expression in posterior mesoderm

Because the phenotype of *fgf8*$^{–}$;*fgf24*^{MO} embryos is similar to that of *spt;ntl* double mutants, we asked if the defects in posterior mesoderm development were associated with defects in the expression of *ntl* and *spt*. We first compared the expression patterns of *ntl* transcripts and Spt protein in eight-somite stage *fgf8*$^{–}$;*fgf24*^{MO} embryos with those of wild-type, *fgf8*$^{–}$ and *fgf24*^{MO} embryos. We found that in comparison with wild-type embryos (Fig. 5A), *fgf8*$^{–}$ (Fig. 5B), but not *fgf24*^{MO} embryos (data not shown), had reduced numbers of Spt protein-expressing cells in the presomitic mesoderm, and nearly 1/3 of the embryos had gaps in the axial mesodermal expression domain of *ntl* (Fig. 5B). Thus, loss of *fgf8* function alone, but not *fgf24*, is sufficient to cause reduced levels of *spt* and *ntl* expression in developing posterior mesoderm, an observation that could explain why *fgf8* single mutants have defects in somitogenesis (Fig. 4C) (Reifers et al., 1998). In contrast to single mutant embryos, we found that all *fgf8*$^{–}$;*fgf24*^{MO} embryos had severe defects in *spt* and *ntl* expression in posterior mesoderm. Although all of *fgf8*$^{–}$;*fgf24*^{MO} embryos had expression of *ntl* in anterior notochord cells (Fig. 4D, Fig. 5C), we could not detect expression of either *ntl* or Spt in more posterior regions (Fig. 5C) (see also supplemental Fig. S1 at http://dev.biologists.org/supplemental/). These data together suggest that *fgf8*$^{–}$;*fgf24*^{MO} embryos at the 10-somite stage do not contain mesodermal precursors in the tail bud.

We next asked at what stage expression of *ntl* and *spt* become dependent on the function of *fgf8* and *fgf24*. We analyzed the expression of *ntl* and *spt* at the beginning of gastrulation, and then again in mid-gastrula stage (8 hpf) embryos. At the beginning of gastrulation, we could not distinguish differences in the expression of the T-box genes in *fgf8*$^{–}$;*fgf24*^{MO} embryos relative to wild-type embryos (data not shown). In mid-gastrula stage embryos, however, we found that *fgf8*$^{–}$;*fgf24*^{MO} embryos had markedly reduced expression of *ntl* relative to wild-type embryos, with the ventral germ ring having the most dramatic reduction (compare Fig. 5D with 5E).

Similarly, we found that *fgf8*$^{–}$;*fgf24*^{MO} embryos had markedly reduced expression of *spt* in both the germ ring and presomitic mesoderm (compare Fig. 5F with 5G). Reducing the activity of *fgf8* or *fgf24* alone did not result in significant decreases in *ntl* or *spt* expression at the embryonic stages analyzed here (data not shown). Thus, cooperative function of *fgf8* and *fgf24* in the germ ring is required for continued high level expression of *ntl* and *spt* in mesodermal precursors, but they are not required for the initial expression of the T-box genes at early gastrula stages.

ntl and *spt* are required for some, but not all, of the expression of *fgf8* and *fgf24* in the germ ring

It had been proposed that Fgf signaling and T-box genes form an auto-regulatory feedback loop, where the expression of one maintains the expression of the other (reviewed by Smith, 1999). We therefore asked what effect loss of *spt* and *ntl* function had on the expression of *fgf8* and *fgf24* during gastrulation. We found that mid-gastrula-stage (8 hpf) *ntl* mutants had reduced expression of both *fgf8* (Fig. 5I) and *fgf24* (Fig. 5M) in axial, but not ventral mesoderm compared with wild-type embryos (Fig. 5H and 5L, respectively). Surprisingly, *spt* mutant embryos also failed to express *fgf8* in axial mesoderm, but had apparently normal expression of *fgf8* in non-axial domains (Fig. 5J). By contrast, expression of *fgf24* in *spt* mutant embryos was reduced ventrally, but not dorsally (Fig. 5N). Finally, we examined the expression of *fgf8* and *fgf24* in *spt;ntl* double mutant embryos, and found that expression levels of *fgf8* were further reduced in the dorsal and lateral but not the ventral, germ ring (Fig. 5K). By contrast, we found that expression of *fgf24* was reduced both dorsally and ventrally, but not laterally in *spt;ntl* double mutants (Fig. 50). These data show that wild-type function of *spt* and *ntl* are required for some, but not all, *fgf8* and *fgf24* expression in mesodermal precursors.

fgf8 interacts with *ntl* and *spt* in vivo

We have so far provided only indirect evidence based on phenotypic analysis and gene expression that interactions between the Fgf ligands Fgf8 and Fgf24, and the T-box genes *spt* and *ntl* are required for posterior mesoderm development in zebrafish. We tested this hypothesis more directly by asking if we could detect genetic interactions between the Fgf ligands and the T-box genes. We therefore constructed and analyzed *fgf8;ntl* and *spt;fgf8* double mutants and used *fgf24*-E3I3 MO to create *fgf24*^{MO};*ntl* and *spt;fgf24*^{MO} mutant embryos. In comparison with wild-type embryos (Fig. 6A), embryos single mutant for either *fgf8* (Fig. 6B) or *ntl* (Fig. 6D) produce significant amounts of paraxial mesoderm, as revealed by the expression of *myod* at the 12-somite stage (Reifers et al., 1998; Halpern et al., 1993). By contrast, we found that *fgf8;ntl* double mutants produced significantly less paraxial mesoderm than would have been expected from simple addition of their single mutant phenotypes (Fig. 6E). Similarly, in comparison with wild-type embryos (Fig. 6K),

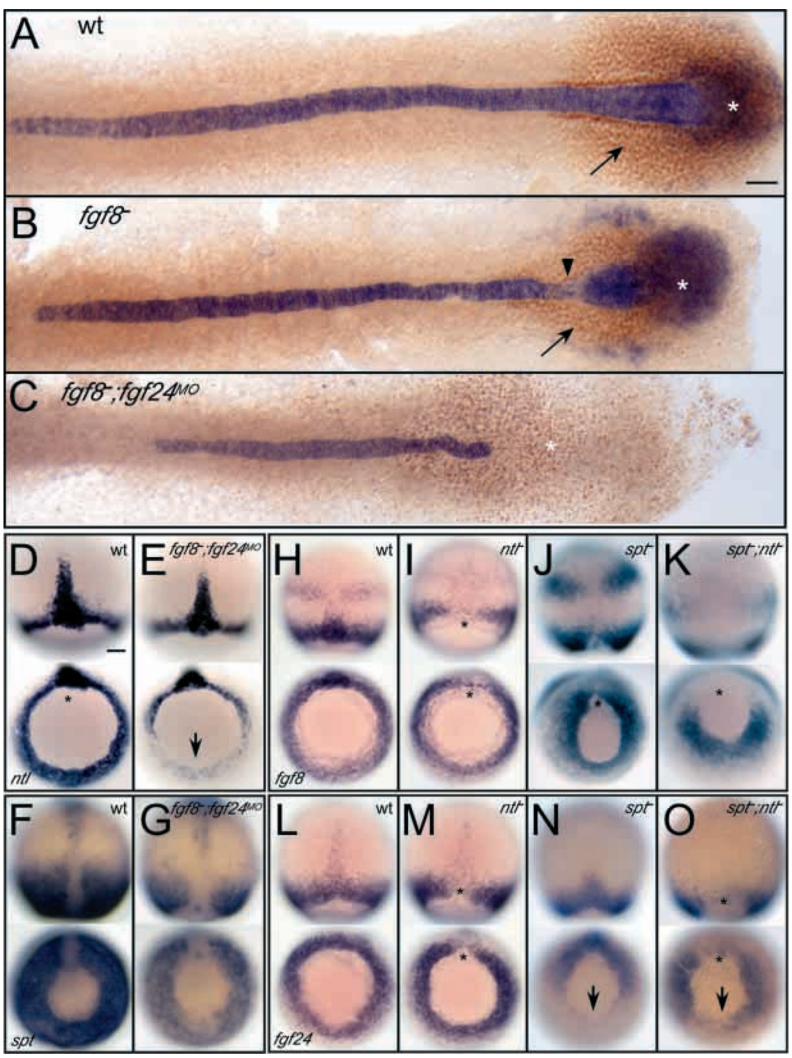

Fig. 5. Fgfs and T-box genes interact during posterior mesoderm development. Expression of *ntl* (purple*)* and Spt (brown) in 10-somite stage wild-type (A), *fgf8* mutant (B) and *fgf8*$^{–}$;*fgf24*^{MO} embryos (C) reveals that *fgf8*$^{–}$;*fgf24*^{MO} embryos no longer have mesodermal precursors that in wild-type (A) and *fgf8* mutants (B) are located in the tail bud (white asterisks) and presomitic mesoderm (arrows). In addition, analysis of these markers reveals that, at this stage, the tail buds of *fgf8* mutant embryos (B) contain significantly less presomitic mesoderm precursors (Spt-expressing cells) in comparison with wild-type embryos (A; see also supplemental Fig. S1 at http://dev.biologists.org/supplemental/), and in the posterior notochord have a gap in the *ntl* expression domain (arrowhead). Dorsal (upper) and vegetal (lower) views showing expression of *ntl* (D,E), *spt* (F,G), *fgf8* (H-K) and *fgf24* (L-O) in mid-gastrula-stage (75-80% epiboly; 8.5 hpf) wild-type and mutant embryos (asterisks and arrows indicate dorsal and ventral tissues, respectively). *fgf8*$^{–}$;*fgf24*^{MO} embryos (E,G) have reduced expression of *ntl* and *spt* in mesodermal precursors relative to wild-type embryos (D,F). Expression of *fgf8* in dorsal mesoderm is reduced in *ntl* (I), *spt* (J) and *spt;ntl* (K) mutant embryos relative to wild-type embryos (H). *fgf24* expression is reduced dorsally in *ntl* embryos (M) ventrally in *spt* embryos (N) and dorsally and ventrally, but not laterally in *spt;ntl* embryos (O), relative to wild-type embryos (L). Scale bars: in A, 50 μm for A-C; in D, 100 μm for D-O.

embryos mutant for either *fgf8* (Fig. 6L) or *spt* (Fig. 6M) produce significant amounts of axial mesoderm, as revealed by the expression of Ntl protein in the nuclei of notochord cells (Fig. 6I-K). By contrast, we found that *spt;fgf8* double mutants produce significantly less axial mesoderm than would have been expected from simple addition of their single mutant phenotypes (Fig. 6N). Fig. 6F-J,O-R give representative examples of live embryos at 24 hpf for each genotypic class (see Materials and methods for segregation frequencies). We did not observe significant differences in the amount of mesoderm produced by either *fgf24*^{MO}*;ntl* or *spt;fgf24*^{MO} embryos when compared with *ntl* or *spt* single mutants, respectively (see supplemental Fig. S2 at http://dev.biologists.org/supplemental/). These data provide direct evidence that *fgf8* genetically interacts with *ntl* and *spt* during the development of posterior mesoderm.

ntl is a dominant enhancer of *fgf8*

When a pair of fish heterozygous for both *ntl* and *fgf8* (i.e. *ntl*$^{+/-}$*;fgf8*$^{+/-}$), are mated, four phenotypic classes are expected [wild type (Fig. 6F), *fgf8* single mutant (Fig. 6G), *ntl* single mutant (Fig. 6I) and *ntl;fgf8* double mutant (Fig. 6J)] that segregate in the ratio of 9:3:3:1, respectively. In this cross, however, we observed that the *fgf8* single mutant class, which was distinguished by lacking the MHB but producing somites and a notochord, could be further sorted into two phenotypic subclasses based on tail length at 24 hpf, or by the amount of notochord produced when assayed for marker gene expression at the 12-somite stage; 1/3 of these embryos were indistinguishable from *fgf8* single mutants (Fig. 6B,G) while 2/3 produced only anterior notochord and had tails that were intermediate in length between *fgf8* single mutants and *fgf8;ntl* double mutants (Fig. 6C,H). Based on these segregation frequencies and the fact that both phenotypic classes produced notochord, we reasoned that the *fgf8* homozygotes that had short tails and reduced notochord development were heterozygous for the *ntl* mutation (i.e. *fgf8*$^{-/-}$*;ntl*$^{+/-}$), whereas those with long tails were *ntl* homozygous wild type (i.e. *fgf8*$^{-/-}$*;ntl*$^{+/+}$). We tested this hypothesis by crossing *fgf8*$^{+/-}$*;ntl*$^{+/-}$ double heterozygous animals to *fgf8*$^{+/-}$ single heterozygotes. In this cross, 1/2 of the *fgf8*$^{-/-}$ embryos will also be genotypically *ntl*$^{+/-}$. Again, we found that we could divide the *fgf8* homozygotes into two phenotypic classes: 1/2 of the *fgf8* mutants segregating in this

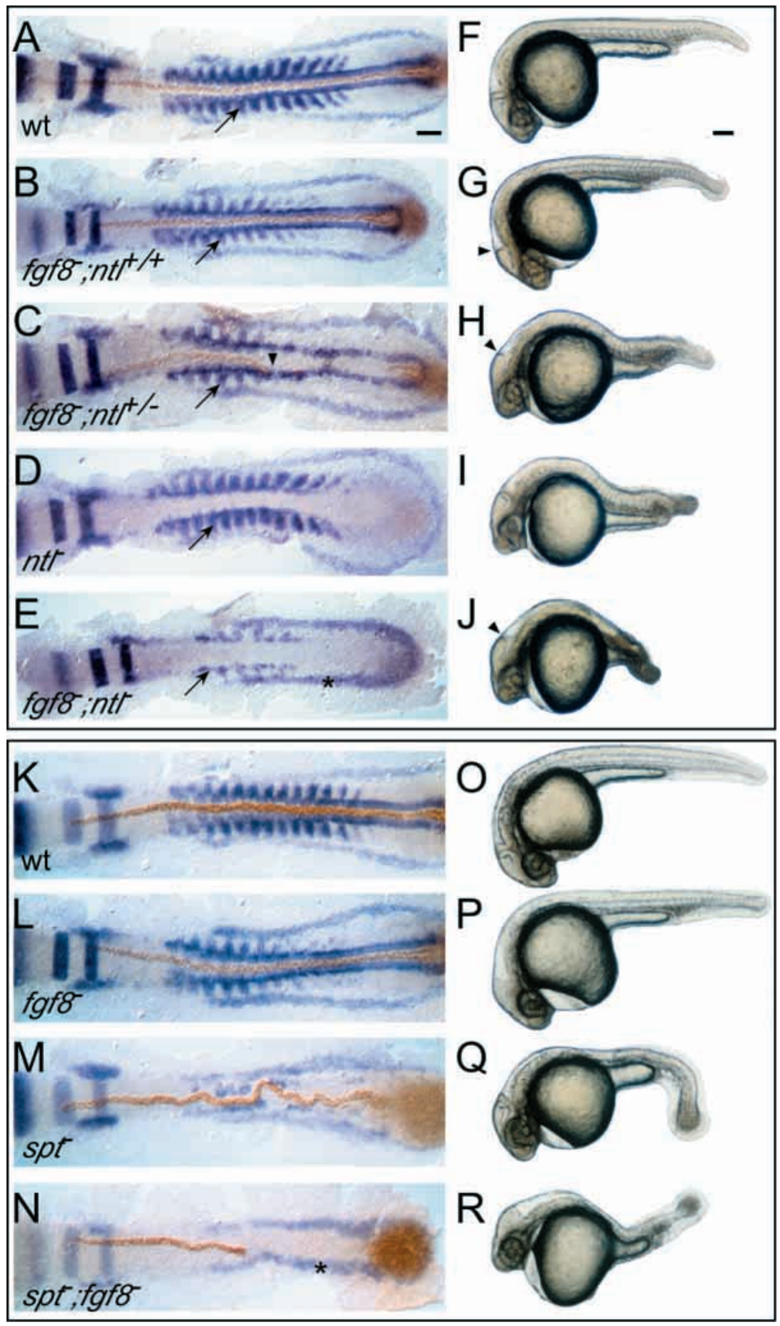

Fig. 6. Double mutant analysis reveals that *fgf8* genetically interacts with *ntl* and *spt*. Markers used for in situ hybridization and immunohistochemistry in A-E and K-N, as well as identifiers (e.g. arrows) are as described for Fig. 4A. Representative pictures of stained 12- to 13-somite-stage embryos (A-E,K-N) and live 24 hpf embryos (F-J,O-R) are shown. Relative to wild-type embryos (A), neither *fgf8* (B) nor *ntl* (D) mutant embryos have severe deficiencies in the production of *myod*-expressing paraxial mesoderm (arrows), whereas *fgf8;ntl* double mutants (E) produce very little paraxial mesoderm and have significantly shorter tails at 24 hpf (J) in comparison with *fgf8* (G) or *ntl* (I) single mutants. By contrast, *fgf8;ntl* double mutants appear to produce relatively normal amounts of pronephric tissue (E; asterisk). In addition to the single and double mutant phenotypes observed, *fgf8*$^{-}$*;ntl*$^{+/-}$ embryos (C) produce less axial (Ntl expressing) and paraxial (*myod* expressing) mesoderm than do *fgf8*$^{-}$*;ntl*$^{+/+}$ embryos (B), and at 24 hpf (H) have tail lengths that are intermediate between embryos single mutant for either *fgf8* (G) or *ntl* (I). Although neither *fgf8* (L) nor *spt* (M) mutant embryos have severe deficiencies in the production of axial mesoderm, *spt;fgf8* double mutant embryos produce a truncated notochord (N) and have shorter tails at 24 hpf (R) than either *fgf8* (P) or *spt* (Q) single mutants. By contrast, *spt;fgf8* double mutants appear to produce relatively normal amounts of pronephric tissue (N; asterisk).Wild-type sibling embryos (K,O) are shown for comparison. Scale bars: in A, 50 μm for A-E,K-N; in F, 100 μm for F-J,O-R.

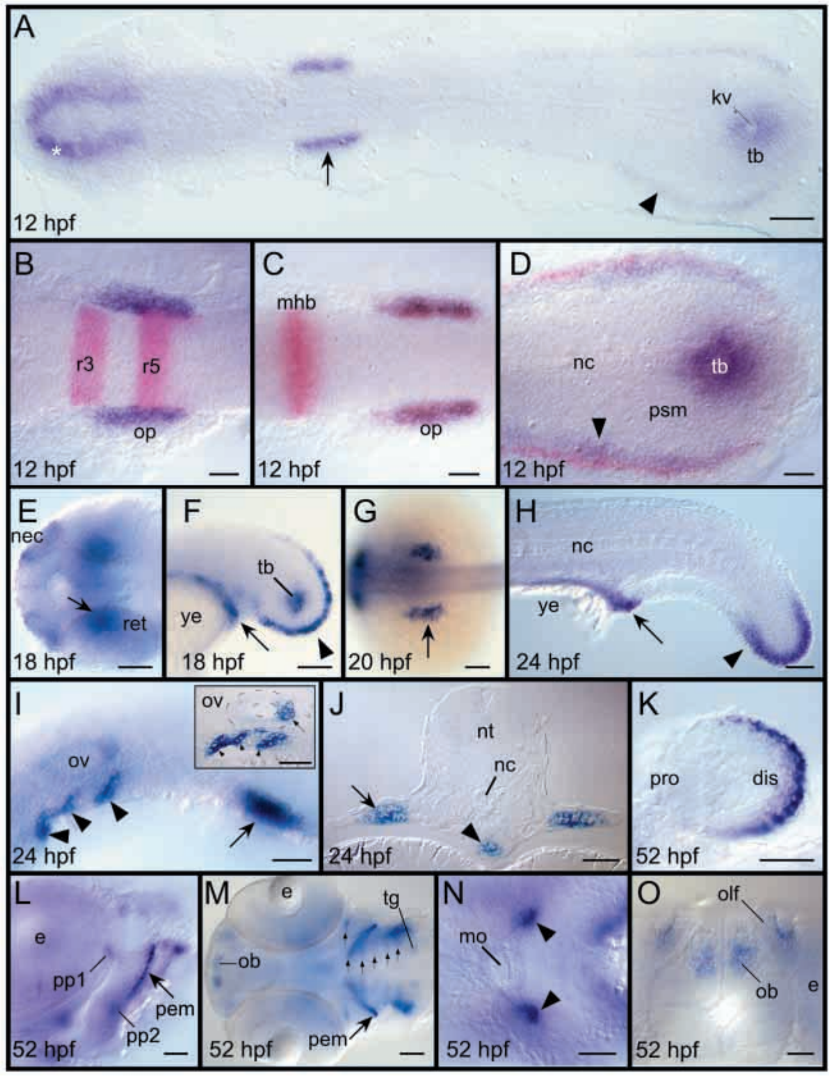

Fig. 7. *fgf24* expression during later embryonic and larval development. In all panels, anterior is towards the left unless specified, and *fgf24* expression is visualized in purple. (A-D) 12 hpf (six-somite stage), dorsal views. (A) *fgf24* is expressed in the nasal placode (asterisk), otic placode (arrow), lateral mesoderm (arrowhead) and tail bud mesenchyme surrounding Kupffer's vesicle. Expression of *fgf24* in the otic placode was confirmed by co-labeling embryos with either *krx20* (red), which labels rhombomere 3 (r3) and r5 (B) or *pax2.1* (red), which labels the otic placode and the mid-hindbrain boundary (C). (D) *fgf24* expression in lateral mesoderm (arrowhead) is in cells that lie adjacent and medial to those expressing *pax2.1* (red). (E,F) 18 hpf. (E) *fgf24* is expressed in nasal ectoderm and in a discrete domain of the retina (arrow, dorsal view). (F) Lateral view of *fgf24*-expressing cells in the posterior gut (arrow), in tail bud mesenchyme and in the caudal fin primordium (arrowhead). (G) 20 hpf, dorsal view. *fgf24*expression in early pectoral fin bud mesenchyme (arrow). (H-J) 24 hpf. (H) *fgf24* expression persists in the posterior gut (arrow) and caudal fin primordium (arrowhead), but is no longer detected in the tail bud (lateral view, yolk extension removed). (I) *fgf24* is expressed in the pharyngeal endoderm (arrowheads) and in the pectoral fin bud mesenchyme (arrow), and in a posterior domain of the otic epithelium (not in focus). Inset in I shows sagittal section through the otic vesicle (outlined), showing more clearly the expression of *fgf24* in the posterior otic epithelium (arrow) and pharyngeal endoderm (arrowheads). (J) Transverse section (dorsal upwards) showing *fgf24* expression in fin bud mesenchyme (arrow) and gut (arrowhead). (K-O) 52 hpf. (K) At this stage, *fgf24* is no longer expressed in pectoral fin mesenchyme, but instead is strongly expressed in the apical ectodermal ridge. (L) Lateral view of head showing *fgf24* expression in the first and second pharyngeal pouches (pp1, ppl2), and the posterior ectodermal margin (pem, arrow) of the second pharyngeal arch. A ventral view (M) shows *fgf24* expression in all pharyngeal pouches (pp1 and pp2-6, small arrows), and the olfactory bulb. Additionally, *fgf24* is expressed in tooth germs, which develop on only the most posterior (seventh) pharyngeal arch. (N) A close-up ventral view shows *fgf24* expression in bilateral domains (arrowheads) adjacent to the lateral edges of the mouth. (O) *fgf24* is expressed in the olfactory organ and the olfactory bulb (dorsal view, anterior is upwards). dis, distal; e, eye; kv, Kupffer's vesicle; mhb, mid-hindbrain boundary; mo, mouth; nec, nasal ectoderm; nc, notochord; nt, neural tube; ob, olfactory bulb; olf, olfactory organ; op, otic placode; ov, otic vesicle; pem, posterior ectodermal margin; psm, presomitic mesoderm; pro, proximal; ret, retina; tb, tail bud; tg, tooth germ; ye, yolk extension. Scale bars: 100 μm in A,G; 50 μm in B-F,H-O.

cross were indistinguishable from *fgf8* single mutants, while the other 1/2 had short tails and patchy notochord, identical to the animals in Fig. 6C,H (see Materials and methods for segregation frequencies). These data show that a loss-of-function *ntl* allele can dominantly enhance the phenotype of *fgf8* mutant embryos, providing further support that *ntl* and *fgf8* interact genetically.

fgf24 expression in later development

After the completion of gastrulation, *fgf24* expression can be detected in a variety of tissues during somitogenesis and larval development. Expression of *fgf24* in the tail bud mesenchyme can be detected in 12-18 hpf embryos (Fig. 7A,D,F), but it is no longer expressed in this domain at 24 hpf (Fig. 7H). *fgf24* is expressed in the otic placode beginning around the two-somite stage (10.5 hpf, not shown) and is clearly visible at 12 hpf (Fig. 7A) as bilateral patches adjacent to rhombomere 5 (Fig. 7B). Co-labeling with the otic placode marker *pax2.1* (Krauss et al., 1991) indicates that *fgf24* is uniformly expressed in the otic placode at 12 hpf (Fig. 7C). Expression of *fgf24* in the developing ear is dynamic and by 24 hpf is localized to a discrete domain in the posterior otic epithelium (Fig. 7I). In addition to the otic placode, *fgf24* is expressed in anterior neuroectoderm at 12 hpf, in a location that has been fate mapped to form the olfactory placode (Fig. 7A) (Whitlock and Westerfield, 2000) and in 18 hpf embryos, expression can be seen in the forming nasal organs (Fig. 7E). Expression of *fgf24* persists in the nasal organ through 52 hpf (the latest time point analyzed), at which point expression can also be detected in the olfactory bubs (Fig. 7M,O). Last, at 12 hpf, *fgf24* expression is detected in bilateral stripes of cells that appear to be located in lateral mesoderm (Fig. 7A). We correlated this expression domain with the expression of *pax2.1*, which at this stage also labels the forming pronephric ducts, an intermediate mesodermal derivative (Krauss et al., 1991), and found that cells expressing *fgf24* lay medial to, and do not appear to overlap with, those expressing *pax2.1* (Fig. 7D). This expression domain may identify precursors of regions of the gut because, at later stages, *fgf24* is also expressed in the developing gut (Fig. 7F,H,J).

Beginning at the 16-somite stage (18 hpf), *fgf24* expression is detected in a restricted domain in the medial retina (Fig. 7E) and in the caudal fin ectoderm (Fig. 7F). Expression in the caudal fin persists through 52 hpf (Fig. 7H and data not shown). Additionally, *fgf24* is detected in bilateral domains of trunk mesoderm beginning at 18 hpf (not shown) which by 20 hpf (Fig. 7G) appear to mark the mesenchyme that will contribute to the developing pectoral fin bud. Thin transverse sections of 24 hpf larva confirm that this expression domain is restricted to the mesenchyme, and not the overlying surface ectoderm (Fig. 7I,J). By 52 hpf, when the developing pectoral fin is clearly visible, *fgf24* expression is no longer detected in the fin mesenchyme, but is instead restricted to the apical ectodermal ridge (Fig. 7K), similar to the expression of *fgf8* (Reifers et al., 1998). At 24 hpf, *fgf24* is also expressed in the pharyngeal pouches (Fig. 7I). In 52 hpf embryos, *fgf24* expression continues in the pharyngeal arches, though the expression domains in the pouches become more restricted to their lateral tips (Fig. 7L-N). Additional pharyngeal arch expression domains are seen as well. For example, in the first arch, *fgf24* is expressed in bilateral patches adjacent to the mouth opening (Fig. 7N), similar to what has been reported for *fgf8* (Reifers et al., 1998). In the second arch, *fgf24* is expressed in the posterior ectodermal margin (Fig. 7M), similar to *fgf8* in chicks (Wall and Hogen, 1998). Last, *fgf24* is expressed in two posterior pharyngeal arch domains that appear to be tooth germs (Fig. 7M). *fgf4*, the mammalian ortholog of which marks a subset of the dental epithelium, is expressed in similar domains at this stage (B.W.D. and D.W.S., unpublished). In zebrafish, as in all cypriniforms, teeth form only on the most posterior (seventh) pharyngeal arch (Kimmel et al., 1995).

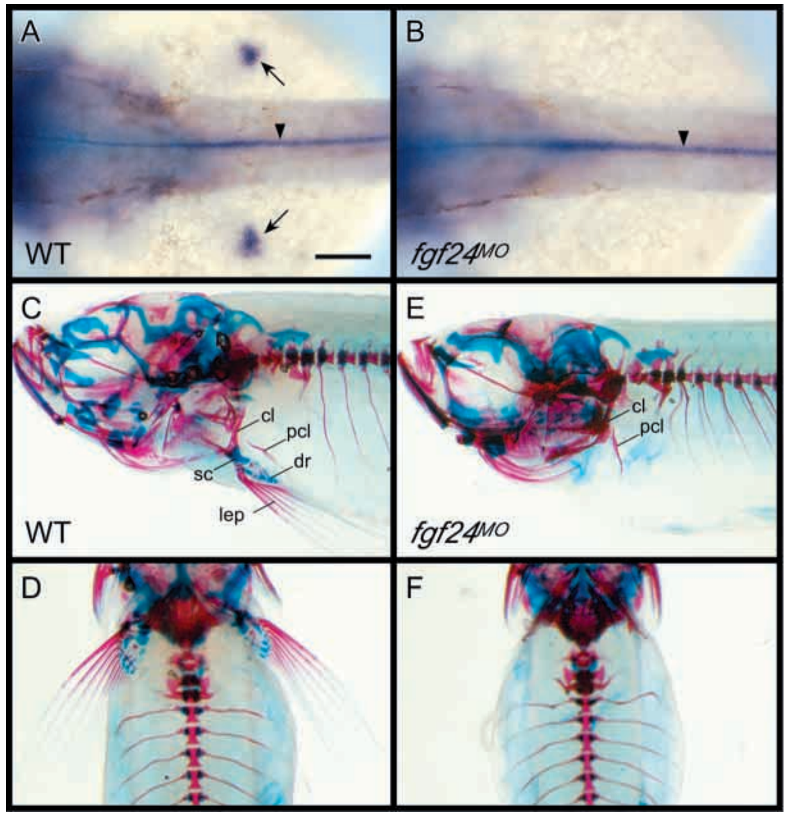

Fig. 8. *fgf24* is required for pectoral fin development. (A,B) Dorsal views of *shh* expression in 24 hpf wild-type (A) and *fgf24*-E3I3 morpholino-injected (B) embryos. *shh* is detected in the pectoral fin buds (arrows) and floor plate (arrowhead) of wild-type embryos (A), but only in the floor plate of *fgf24*-E3I3 morpholino-injected embryos (B). Skeletal preparations of one-month-old wild-type (C,D) and *fgf24*-E3I3 morpholino-injected fish (E,F) shown in lateral (C,E) and ventral (D,F) views. Bone is stained red and cartilage blue. In wild-type fish, exoskeletal (cleithrum and postcleithrum) and endoskeletal (scapula, distal radials and lepidotrichs) components of the pectoral fin are visible (C). By contrast, only exoskeletal components can be identified in *fgf24*-E3I3 injected fish (E). cl, cleithrum; dr, distal radials; lep, lepidotrichs; pcl, postcleithrum; sc, scapula. Scale bar: in A, 50 μm for A,B.

fgf24 is required for pectoral fin formation

We used the *fgf24*-E3I3 MO to address the function of *fgf24* in later development. As shown previously, *fgf24*^{MO} embryos at 24 hpf are morphologically indistinguishable from their control siblings (Fig. 3E,F). We therefore allowed *fgf24*^{MO} embryos to develop to various stages past 24 hpf, and assayed for morphological phenotypes. We found that at 33 hpf, *fgf24*^{MO} embryos were indistinguishable form their control sibling embryos, with the exception that they did not have visible pectoral fin buds, which are easily scored at this stage of development as discrete epidermal bumps on the dorsal yolk (not shown) (Kimmel et al., 1995; Grandel and Schulte-Merker, 1998), or by their expression of *shh* (Fig. 8A,B) (Krauss et al., 1993). Surprisingly, we found that injected embryos could survive to adulthood, but they never develop pectoral fins.

We investigated the pectoral fin phenotype in more detail by analyzing skeletal preparations of 1-month-old wild-type and *fgf24*^{MO} fish stained with Alizarin Red and Alcian Green to visualize bone and cartilage, respectively. The skeleton of the paired pectoral fins in zebrafish consist of fin rays or lepidotrichia, that support the visible part of the fin, and a pectoral girdle located internally that provides support for the fin rays as well as articulation with the skull (Grandel and Schulte-Merker, 1998). We analyzed pectoral skeletal morphology in wild-type (Fig. 8C,D) and *fgf24*^{MO} fish (Fig. 8E,F) and found that elements of the pectoral girdle, the cleithrum and postcleithrum, could be found in both wild-type and *fgf24*^{MO} fish. By contrast, elements derived from the fin bud (i.e. scapula, radials and lepidotrichia) could only be identified in wild-type (Fig. 8C), but not in *fgf24*^{MO} fish (Fig. 8E). Thus, loss of *fgf24* function appears to affect a very early stage of pectoral fin development. A more detailed analysis of the role of *fgf24* in pectoral fin development is presented elsewhere (Fischer et al., 2003).

Discussion

We have described the identification and function of zebrafish *fgf24*, a new member of the fibroblast growth factor (Fgf) 8/17/18 subfamily of signaling molecules. Our results show that *fgf24* is expressed in posterior mesodermal precursors during gastrulation where it functions cooperatively with *fgf8* to promote mesodermal development, in part by maintaining the expression of the mesodermal T-box genes *ntl* and *spt*. We have presented double mutant analyses that reveal genetic interactions between the T-box genes and Fgf signaling. These results provide compelling evidence that these genes function in a genetic pathway that promotes posterior mesodermal development in zebrafish. Last, we have shown that *fgf24* is expressed in a wide variety of tissues after gastrulation, including the early fin bud mesenchyme, and is required for an early stage of pectoral fin bud development.

fgf24 and its relationship to the *fgf8/17/18* subfamily of Fgf ligands

With the addition of *fgf24*, at least 22 distinct Fgf-encoding genes have been identified in vertebrates (human *FGF19* and mouse *Fgf15* may be orthologous genes). Based on sequence relatedness, the Fgf superfamily can be subdivided into seven subfamilies of more closely related genes (reviewed by Ornitz and Itoh, 2001). The genes encoding the ligands *Fgf8*, *Fgf17*, *Fgf18*, and Fgf24 define one such subfamily and mouse members of this subfamily have been shown to have very similar Fgf receptor specificity profiles (Xu et al., 2000). It is therefore likely that in zebrafish Fgf8 and Fgf24 have similar activities.

Because Fgf24 so far appears to be unique to zebrafish, it is necessary to consider its origin. There is increasing evidence that a whole-genome duplication event occurred in the ray-finned fish lineage after it diverged form the terrestrial vertebrate lineage (Amores et al., 1998; Postlethwait et al., 1998; Force et al., 1999; Postlethwait et al., 2000). It is therefore possible that *fgf18* and *fgf24* are paralogs that arose by duplication of an ancestral *fgf18* during this proposed event. However we have shown that *fgf24* and *fgf18* are closely linked on LG14, whereas paralogs that resulted from a genome duplication event are expected to be unlinked (see Woods et al., 2000). In addition, we found compelling evidence of conserved gene synteny around the zebrafish and human Fgf18 loci. By contrast, the *fgf24* locus does not appear to be in a region with conserved synteny with any region of the human genome. Finally, the grouping of zebrafish Fgf24 with zebrafish Fgf18 is contradicted by a node with 97% bootstrap support in our phylogenetic analysis of Fgf protein sequences. Thus, our data argues that *fgf24* and *fgf18* are not paralogous genes that resulted from the ray-finned fish-specific genome duplication.

We instead favor the model that *fgf24* and *fgf18* are paralogs that resulted from a gene duplication event that predates the divergence of ray-finned fish and terrestrial vertebrate lineages. Based on protein sequence relatedness, Fgf24 is as similar to *Fgf18* orthologs, as *Fgf17* orthologs are to *Fgf8*. It is therefore possible that a single ancestral gene, following two sequential duplication events, gave rise to the four members of the *Fgf8* subfamily. A similar hypothesis has been proposed for the origin of the four tetapod Hox clusters (discussed by Furlong and Holland, 2001). In support of this model, a probable *fgf24* ortholog has been identified in a shark (D.W.S., unpublished), arguing that *fgf24* arose early in gnathostome (jawed vertebrate) evolution. It is therefore likely that an *fgf24* ortholog was lost at some point in the terrestrial vertebrate lineage after its divergence from ray-finned fishes. Similar examples of lineage-specific gene loss have already been described, including the loss of functional copies of the *hox* paralogs *hoxb10*, *hoxc1* and *hoxc3* in the mammalian lineage, but not in zebrafish (Amores et al., 1998; Prince et al., 1998; Postlethwait et al., 1998).

Fgf8 and Fgf24 are components of the Fgf signaling pathway that is required for posterior mesoderm development in zebrafish

Our results show that *fgf8* and *fgf24* are components of the Fgf signaling pathway that regulates posterior mesoderm development in zebrafish. We found that *fgf8* and *fgf24* are expressed in mesodermal precursors and that *fgf8*$^{-}$;*fgf24*^{MO} embryos produce very little posterior mesoderm. Although the function of *fgf8* and *fgf24* can account for much of the Fgf signaling activity that is known to be required for posterior mesoderm development in zebrafish, we observed that *fgf8*$^{-}$;*fgf24*^{MO} embryos produce significantly more mesoderm than do embryos overexpressing the dnFgfr (Griffin et al., 1995). Because the dnFgfr is likely to block all Fgf signaling in early embryos (Ueno et al., 1992), ligands in addition to Fgf8 and Fgf24 are likely to contribute to early mesoderm formation in zebrafish. In addition to *fgf8* and *fgf24*, *fgf3* is the only other Fgf gene in zebrafish that is known to be expressed in mesodermal precursors during gastrulation (Fürthauer et al., 2001). Although *fgf3* may account for some of the Fgf activity present in *fgf8*$^{-}$;*fgf24*^{MO} embryos, it is not likely to account for all; injection of *fgf3* MO (Maves et al., 2002) into *fgf8*$^{-}$;*fgf24*^{MO} embryos does not appear to decrease the amount of posterior mesoderm produced relative to *fgf8*$^{-}$;*fgf24*^{MO} embryos alone (L. Maves and B.W.D., unpublished).

We cannot rule out the possibility that the mesoderm produced by *fgf8*$^{-}$;*fgf24* ^{MO} embryos is due to residual activity of *fgf8* and/or *fgf24* in these embryos. The single *fgf8* allele that has been isolated, *fgf8*^{ti282} (Reifers et al., 1998), is likely to be a hypomorph (Draper et el., 2001). However, using *fgf8* MOs, which reduce the expression of functional *fgf8* below the level produced by the *fgf8* mutation (Draper et al., 2001), in combination with the *fgf24* MO, does not appear to increase the severity of the phenotype relative to the *fgf8*$^{-}$;*fgf24*^{MO} embryos (B.W.D., unpublished). Similarly, it is possible that our *fgf24* MO does not completely eliminate *fgf24* function, although our RNase protection results argue against this. Last, *fgf8* (Reifers et al., 1998; Draper et al., 2001), *fgf24* and *fgf18* (this study) are expressed maternally and these maternal mRNAs persist for several hours after fertilization. It is therefore possible that sufficient amounts of Fgf protein are produced from wild-type maternal transcripts to allow partial mesoderm development in the absence of zygotic *fgf8* and *fgf24* function. As only a few orthologs of the known vertebrate Fgf ligands have been identified in zebrafish, it remains to be seen how many other ligands participate in posterior mesodermal development.

Fgf8 and Fgf24 maintain *spt* and *ntl* expression during posterior development

Current models for how Fgfs and T-box genes interact during mesodermal development have proposed that they form an auto-regulatory feedback loop, where the function of one component maintains the expression of the other (reviewed by Isaacs, 1997). Although it is not yet clear how Fgf signaling regulates T-box gene expression, there is evidence in *Xenopus* that *Xbra*, the ortholog of *ntl*, can directly regulate the expression of embryonic (*e*)*Fgf*, an *Fgf4* ortholog (Casey et al., 1998). This model predicts that wild-type expression patterns of *fgf8* and *fgf24* should require *ntl* and *spt* function, and indeed we found this to be true. However, *ntl* and *spt* can not be the only regulators of *fgf8* and *fgf24* expression during early mesoderm formation, as expression of *fgf8* and *fgf24* persist in the germ ring of early *spt;ntl* double mutant embryos. In addition to *spt* and *ntl*, the *spt*-related gene *tbx6* is also expressed in mesodermal precursors during gastrulation (Hug et al., 1997). *tbx6* is unlikely to contribute to Fgf regulation in the absence of *spt* and *ntl* function, however, because it is not expressed in *spt;ntl* double mutants (Griffin et al., 1998).

The expression patterns we observed for *fgf8* and *fgf24* in wild-type embryos and in embryos mutant for either *ntl* or *spt* suggest that their expression in the germ ring is not regulated by an identical genetic network. First, the expression patterns of *fgf8* and *fgf24* in wild-type embryos, while overlapping, are not identical. We found that cells expressing the highest levels of *fgf8* localize to the epiblast layer (similar to *ntl*), whereas those expressing the highest levels of *fgf24* localize to the hypoblast layer (similar to *spt*). As might be expected from these expression patterns, expression of *fgf8* and *fgf24* also have non-identical requirements for *ntl* and *spt* function. However, we did not observe a simple one-to-one correlation between an Fgf expression domain and a T-box gene. Instead, we found that the expression of *fgf8* in dorsal mesodermal precursors requires both *ntl* and *spt* function, while neither gene was required for *fgf8* expression in ventral precursors. By contrast, expression of *fgf24* in dorsal mesodermal precursors requires *ntl*, but not *spt*, whereas ventral expression requires *spt*, but not *ntl*. Although it is not possible at present to derive an accurate pathway that explains the regulatory relationships that exist between these Fgfs and T-box genes, our data are consistent with the proposed feedback loop because we have found that reduction of Fgf signaling leads to a reduction of T-box gene expression and vice versa.

fgf8 genetically interacts with *ntl* and *spt*

Data supporting the model that posterior development is promoted by a regulatory network between Fgfs and T-box genes has come largely from analyzing gene expression defects in single mutant embryos (e.g. Yamaguchi et al., 1994; Deng et al., 1994; Sun et al., 1999) or in embryos overexpressing single network components (e.g. Isaacs et al., 1994; Schulte-Merker and Smith, 1995). We have provided genetic evidence that directly links Fgf signaling and T-box gene function in a genetic pathway that promotes posterior development. We have shown that *fgf8;ntl* and *spt;fgf8* double mutants had phenotypes that were more severe than would be expected from the simple addition of either single mutant phenotype. For example, neither *fgf8* nor *ntl* has severe defects in trunk somite formation, as assayed by *myod* expression, whereas *fgf8;ntl* double mutants produce few *myod*-positive cells. Because trunk somite formation is known to require *spt* function cell-autonomously (Ho and Kane, 1990), we propose that the muscle phenotype observed in *fgf8;ntl* embryos results from attenuated *spt* function. Similarly, we found that *spt;fgf8* double mutant embryos appear to have attenuated *ntl* function as notochord development was reduced in double mutant embryos, but not in *spt* or *fgf8* single mutant embryos. These results indicate that *fgf8* cooperates with *ntl* to maintain *spt* function, and similarly with *spt* to maintain *ntl* function.

It is interesting that the expression of *pax2.1*, which marks the developing pronephric tubules (Krauss et al., 1991), is largely unaffected in either *fgf8;ntl* or *spt;fgf8* mutants. Pronephric tubules develop from intermediate mesoderm and *spt* and *ntl* are redundantly required for their formation (Amacher et al., 2002). It is possible that pronephric development requires lower levels of T-box gene activity relative to that required for the development of the notochord and somites. Alternatively, Fgf8 signaling may promote the expression of dorsal-specific factors that function in combination with *ntl* and *spt* to promote the development of dorsal mesodermal derivatives, such as notochord and somites, but not the development of more intermediate derivatives, such as pronephros. In support of this, *fgf8* is expressed at higher levels in dorsal mesoderm than ventral mesoderm and *fgf8* overexpression can strongly dorsalize early zebrafish embryos (Fürthauer et al., 1997).

In addition to the interactions described above, we found that *ntl* mutations dominantly enhance the phenotype of *fgf8* homozygotes: *fgf8*$^{-/-}$;*ntl*$^{+/-}$ embryos produced less posterior mesoderm than *fgf8*$^{-/-}$;*ntl*$^{+/+}$ embryos. Because *ntl* heterozygotes alone are phenotypically wild type, this result suggests that *ntl* function is attenuated in *fgf8* single mutants, and consistent with this, we found that a third of the *fgf8* single mutants have reduced *ntl* expression in axial mesoderm. These results imply that in the absence of *fgf8* function, *fgf24* function alone is not sufficient to maintain wild-type levels of *ntl* activity. Interestingly, *T* null mutations in mice, but not in zebrafish, are semi-dominant as *T*$^{+/-}$ heterozygotes have shorter tails than do wild-type mice (Dobrovolskaïa-Zavadskaïa, 1927). Because wild-type expression of *T* in mouse mesodermal precursors is known to be dependent on *Fgf8* function (Sun et al., 1999), it is possible that the apparent differences between the phenotypes of *T/ntl* heterozygotes in mice and zebrafish are due simply to differences in the quantitative levels of Fgf signaling in posterior tissue between these two organisms. In contrast to dominant interactions between *ntl* and *fgf8*, we could not find evidence that reduction of *spt* function could dominantly enhance the phenotype of *fgf8* mutant embryos, suggesting that the interactions between *fgf8* and *ntl* are stronger than those between *fgf8* and *spt*. Genetic interactions between the Fgf signaling pathway and T-box transcription factors is becoming a common theme in vertebrate development, as similar interactions have been proposed to play key roles in development of limbs (Ng et al, 2002) the cardiovascular system (Vitelli et al., 2002) and lungs (Cebra-Thomas et al., 2003).

Fgf24 is required for pectoral fin development

Last, we have shown that *fgf24* expression is not restricted to developing posterior mesoderm, but is also expressed in a wide variety of tissues during larval growth. However, the only defect we could identify in *fgf24^{MO}* embryos was in the development of pectoral fins. We found that *fgf24^{MO}* fish never produced a morphological fin bud, nor did they produce any skeletal elements of the external pectoral fin. Thus, the phenotype of *fgf24* appears similar to that of mice mutant for either *fgf10* (Min et al., 1998; Sekine et al., 1998) or its likely receptor, *Fgfr2* (Xu et al., 1998).

We thank Thierry Lepage and David Kimelman for generously sharing their cDNA library; Karen Larison and Jewel Parker for expert sectioning assistance; Brian Summers for excellent technical assistance; Angel Amores for help with PAC library screening; Craig Miller for assistance identifying expression domains in larva and for many thoughtful discussions; members of the Kimmel laboratory for thoughtful discussions; The University of Oregon Zebrafish Facility for excellent fish care; David Kimelman, Cecilia Moens, Craig Miller and Lisa Maves for excellent comments on the manuscript; and Kenneth Weiss for research support of D.W.S. This work was supported by the NIH (5 PO1 HD22486 to C.B.K.), the Damon Runyon Cancer Research Foundation (B.W.D.) and the NSF (SBR 9408402 to K. M. Weiss).

References

Amacher, S. L., Draper, B. W., Summers, B. R. and Kimmel, C. B. (2002). The zebrafish T-box genes no tail and spadetail are required for development of trunk and tail mesoderm and medial floor plate. *Development* **129**, 3311-3323.

Amaya, E., Musci, T. J. and Kirschner, M. W. (1991). Expression of a dominant negative mutant of the FGF receptor disrupts mesoderm formation in Xenopus embryos. *Cell* **66**, 257-270.

Amaya, E., Stein, P. A., Musci, T. J. and Kirschner, M. W. (1993). FGF signaling in the early specification of mesoderm in Xenopus. *Development* **118**, 477-487.

Amemiya, C. T. and Zon, L. I. (1999). Generation of a zebrafish P1 artificial chromosome library. *Genomics* **58**, 211-213.

Amores, A., Force, A., Yan, Y. L., Joly, L., Amemiya, C., Fritz, A., Ho, R. K., Langeland, J., Prince, V., Wang, Y. L. et al. (1998). Zebrafish hox clusters and vertebrate genome evolution. *Science* **282**, 1711-1714.

Araki, I. and Brand, M. (2001). Morpholino-induced knockdown of *fgf8* efficiently phenocopies the acerebellar (ace) phenotype. *Genesis* **30**, 157-159.

Casey, E. S., O'Reilly, J. M.-A., Conlon, F. L. and Smith, J. C. (1998). The T-box transcription factor Brachyury regulates expression of *eFGF* through binding to a non-palindromic response element. *Development* **125**, 3887-3894.

Cebra-Thomas, J. A., Bromer, J., Gardner, R., Lam, G. K., Sheipe, H. and Gilbert, S. F. (2003). T-box gene products are required for mesenchymal induction of epithelial branching in the embryonic mouse lung. *Dev Dyn*. **226**, 82-90.

Ciruna, B. G., Schwartz, L., Harpal, K., Yamaguchi, T. P. and Rossant, J. (1997). Chimeric analysis of fibroblast growth factor receptor-1 (Fgfr1) function: a role for FGFR1 in morphogenetic movement through the primitive streak. *Development* **124**, 2829-2841.

Ciruna, B. and Rossant, J. (2001). FGF signaling regulates mesoderm cell fate specification and morphogenetic movement at the primitive streak. *Dev Cell.* **1**, 37-49.

Conlon, F. L., Sedgwick, S. G., Weston, K. M. and Smith, J. C. (1996). Inhibition of Xbra transcription activation causes defects in mesodermal patterning and reveals autoregulation of Xbra in dorsal mesoderm. *Development* **122**, 2427-2435.

Crossley, P. H. and Martin, G. R. (1995). The mouse Fgf8 gene encodes a family of polypeptides and is expressed in regions that direct outgrowth and patterning in the developing embryo. *Development* **121**, 439-451.

Cunliffe, V. and Smith, J. C. (1992). Ectopic mesoderm formation in Xenopus embryos caused by widespread expression of a Brachyury homologue. *Nature* **358**, 427-430.

Davis, R. L. and Kirschner, M. W. (2000). The fate of cells in the tail bud of Xenopus laevis. *Development* **127**, 255-267.

Deng, C. X., Wynshaw-Boris, A., Shen, M. M., Daugherty, C., Ornitz, D. M. and Leder, P. (1994). Murine FGFR-1 is required for early postimplantation growth and axial organization. *Genes Dev.* **8**, 3045-3057.

Dobrovolskaïa-Zavadskaïa, N. (1927). Sur la mortification spontanée de la queue la souris nouveau-née et sur l'existence d'un caractère (facteur) héréditaire 'non-viable'. *C. R. Seanc. Soc. Biol.* **97**, 114-116.

Draper, B. W., Morcos, P. A. and Kimmel, C. B. (2001). Inhibition of zebrafish *fgf8* pre-mRNA splicing with morpholino oligos: a quantifiable method for gene knockdown. *Genesis* **30**, 154-156.

Drucker, B. J. and Goldfarb, M. (1993). Murine FGF-4 gene expression is spatially restricted within embryonic skeletal muscle and other tissues. *Mech. Dev*. **40**, 155-163.

Feldman, B., Poueymirou, W., Papaioannou, V. E., DeChiara, T. M. and Goldfarb, M. (1995). Requirement of FGF-4 for postimplantation mouse development. *Science* **267**, 246-249.

Fischer, S., Draper, B. W. and Neumann C. J. (2003). The zebrafish *fgf24* mutant identifies an additional level of Fgf signaling involved in vertebrate limb initiation *Development* **130**, 3515-3524.

Force, A., Lynch, M., Pickett, F. B., Amores, A., Yan, Y. L. and Postlethwait, J. (1999). Preservation of duplicate genes by complementary, degenerative mutations. *Genetics* **151**, 1531-1545.

Furlong, R. F. and Holland, P. W. H. (2001). Were vertebrates octoploid? *Philos. Trans. R. Soc. Lond. B. Biol. Sci.* **357**, 531-544.

Fürthauer, M., Thisse, C. and Thisse, B. (1997). A role for FGF-8 in the dorsoventral patterning of the zebrafish gastrula. *Development* **124**, 4253-4264.

Fürthauer, M., Reifers, F., Brand, M., Thisse, B. and Thisse, C. (2001). sprouty4 acts in vivo as a feedback-induced antagonist of FGF signaling in zebrafish. *Development* **128**, 2175-2186.

Geisler, R., Rauch, G. J., Baier, H., van Bebber, F., Brobeta, L., Dekens, M. P., Finger, K., Fricke, C., Gates, M. A., Geiger, H. et al. (1999). A radiation hybrid map of the zebrafish genome. *Nat. Genet.* **23**, 86-89.

Grandel, H. and Schulte-Merker, S. (1998). The development of the paired fins in the zebrafish (Danio rerio). *Mech. Dev.* **79**, 99-120.

Griffin, K., Patient, R. and Holder, N. (1995). Analysis of FGF function in normal and no tail zebrafish embryos reveals separate mechanisms for formation of the trunk and the tail. *Development* **121**, 2983-2994.

Griffin, K. J., Amacher, S. L., Kimmel, C. B. and Kimelman, D. (1998). Molecular identification of spadetail: regulation of zebrafish trunk and tail mesoderm formation by T-box genes. *Development* **125**, 3379-3388.

Halpern, M. E., Ho, R. K., Walker, C. and Kimmel, C. B. (1993). Induction of muscle pioneers and floor plate is distinguished by the zebrafish no tail mutation. *Cell* **75**, 99-111.

Haub, O. and Goldfarb, M. (1991). Expression of the fibroblast growth factor-5 gene in the mouse embryo. *Development* **112**, 397-406.

Hébert, J. M., Boyle, M. and Martin, G. R. (1991). mRNA localization studies suggest that murine fibroblast growth factor-5 plays a role in gastrulation. *Development* **112**, 407-415.

Hébert, J. M., Rosenquist, T., Götz, J. and Martin, G. R. (1994). FGF5 as a regulator of the hair growth cycle: evidence from targeted and spontaneous mutations. *Cell* **78**, 1017-1025.

Heikinheimo, M., Lawshe, A., Shackleford, G. M., Wilson, D. B. and MacArthur, C. A. (1994). Fgf-8 expression in the post-gastrulation mouse suggests roles in the development of the face, limbs and central nervous system. *Mech. Dev.* **48**, 129-138.

Herrmann, B. G., Labeit, S., Poustka, A., King T. R. and Lehrach, H. (1990). Cloning of the T gene required in mesoderm formation in the mouse. *Nature* **343**, 617-622.

Ho, R. K. and Kane, D. A. (1990). Cell-autonomus action of the zebrafish *spt-1* mutation in specifying mesodermal precursors. *Nature* **348**, 728-730.

Horb, M. E. and Thomsen, G. H. (1997). A vegetally localized T-box transcription factor in *Xenopus* eggs specifies mesoderm and endoderm and is essential for embryonic mesoderm formation. *Development* **124**, 1689-1698.

Hu, M. C.-T., Wang, Y. and Qiu, W. R. (1999). Human fibroblast growth factor-18 stimulates fibroblast cell proliferation and is mapped to chromosome 14p11. *Oncogene* **18**, 2635-2642.

Hug, B., Walter, V. and Grunwald, D. J. (1997). tbx6, a Brachyury-related gene expressed by ventral mesendodermal precursors in the zebrafish embryo. *Dev. Biol.* **183**, 61-73.

Isaacs, H. V. (1997). New perspectives on the role of the fibroblast growth factor family in amphibian development. *Cell. Mol. Life Sci*. **53**, 350-361.

Isaacs, H. V., Pownall, M. E. and Slack, J. M. (1994). eFGF regulates Xbra expression during Xenopus gastrulation. *EMBO J*. **13**, 4469-4481.

Kanki, J. P. and Ho, R. K. (1997). The development of the posterior body in zebrafish. *Development* **124**, 881-893.

Kimmel, C. B., Kane, D. A., Walker, C., Warga, R. M. and Rothman, M. B. (1989). A mutation that changes cell movement and cell fate in the zebrafish embryo. *Nature* **337**, 358-362.

Kimmel, C. B., Warga, R. M. and Schilling, T. F. (1990). Origin and organization of the zebrafish fate map. *Development* **108**, 581-594.

Kimmel, C. B., Ballard, W. W., Kimmel, S. R., Ullmann, B. and Schilling, T. F. (1995). Stages of embryonic development of the zebrafish. *Dev. Dyn.* **203**, 253-310.

Krauss, S., Johansen, T., Korzh, V. and Fjose, A. (1991). Expression of the zebrafish paired box gene pax[zf-b] during early neurogenesis. *Development* **113**, 1193-1206.

Krauss, S., Concordet, J. P. and Ingham, P. W. (1993). A functionally conserved homolog of the Drosophila segment polarity gene hh is expressed in tissues with polarizing activity in zebrafish embryos. *Cell* **75**, 1431-1444.

Kwok, C., Korn, R. M., Davis, M. E., Burt, D. W., Critcher, R., McCarthy, L., Paw, B. H., Zon, L. I., Goodfellow, P. N. and Schmitt, K. (1998). Characterization of whole genome radiation hybrid mapping resources for non-mammalian vertebrates. *Nucleic Acids Res.* **26**, 3562-3566.

Lustig, K. D., Kroll, K. L., Sun, E. E. and Kirschner, M. W. (1996). Expression cloning of a *Xenopus* T-related gene (*Xombi*) involved in mesodermal patterning and blastopore lip formation. *Development* **122**, 4001-4012.

Mansour, S. L., Goddard, J. M. and Capecchi, M. R. (1993). Mice homozygous for a targeted disruption of the proto-oncogene *int-2* have developmental defects in the tail and inner ear. *Development* **117**, 13-28.

Martin, G. R. (1998). The role of FGFs in the early development of the vertebrate limb. *Genes Dev.* **12**, 1571-1586.

Maves, L., Jackman, W. and Kimmel, C. B. (2002). FGF3 and FGF8 mediate a rhombomere 4 signaling activity in the zebrafish hindbrain. *Development* **29**, 3825-3837.

Min, H., Danilenko, D. M., Scully, S. A., Bolon, B., Ring, B. D., Tarpley, J. E., DeRose, M. and Simonet, W. S. (1998). Fgf-10 is required for both limb and lung development and exhibits striking functional similarity to Drosophila branchless. *Genes Dev.* **12**, 3156-3161.

Nasevicicius, A. and Ekker, S. C. (2000). Effective targeted gene 'knockdown' in zebrafish. *Nat. Genet.* **26**, 216-220.

Ng, J. K., Kawakami, Y., Buscher, D., Raya, A., Itoh, T., Koth, C. M., Rodriguez Esteban, C., Rodriguez-Leon, J., Garrity, D. M., Fishman, M. C. and Izpisua Belmonte, J. C. (2002). The limb identity gene Tbx5 promotes limb initiation by interacting with Wnt2b and Fgf10. *Development* **129**, 5161-5170.

Nielsen, H., Engelbrecht, J., Brunak, S. and von Heijne, G. (1997). Identification of prokaryotic and eukaryotic signal peptides and prediction of their cleavage sites. *Prot. Engineering* **10**, 1-6.

Niswander, L. and Martin, G. R. (1992). Fgf-4 expression during gastrulation, myogenesis, limb and tooth development in the mouse. *Development* **114**, 755-768.

Ohbayashi, N., Hoshikawa, M., Kimura, S., Yamasaki, M., Fukui, S. and Itoh, N. (1998). Structure and expression of the mRNA encoding a novel fibroblast growth factor, FGF-18. *J. Biol. Chem.* **273**, 18161-18164.

Ohuchi, H., Yoshioka, H., Tanaka, A., Kawakami, Y., Nohno, T. and Noji, S. (1994). Involvement of androgen-induced growth factor (FGF-8) gene in mouse embryogenesis and morphogenesis. *Biochem. Biophys. Res. Commun*. **204**, 882-888.

O'Reilly, M. A., Smith, J. C. and Cunliffe, V. (1995). Patterning of the mesoderm in *Xenopus*: dose-dependent and synergistic effects of *Brachyury* and *Pintallavis*. *Development* **121**, 1351-1359.

Ornitz, D. M. and Itoh, N. (2001). Fibroblast growth factors. *Genome Biol.* **2**, 2-12.

Oxtoby, E. and Jowett, T. (1993). Cloning of the zebrafish krox-20 gene (krx-20) and its expression during hindbrain development. *Nucleic Acids Res.* **21**, 1087-1095.

Papaioannou, V. E. (2001). T-box genes in development: from hydra to humans. *Int. Rev. Cytol.* **207**, 1-70.

Postlethwait, J. H, Yan, Y.-L., Gates, M. A., Horne, S., Amores, A., Brownlie, A., Donovan, A., Egan, E. S., Force, A., Gong, Z. et al. (1998). Vertebrate genome evolution and the zebrafish gene map. *Nat. Genet.* **18**, 345-349.

Postlethwait, J. H., Woods, I. G., Ngo-Hazelett, P., Yan, Y. L., Kelly, P. D., Chu, F., Huang, H., Hill-Force, A. and Talbot, W. (2000). Zebrafish comparative genomics and the origin of vertebrate chromosomes. *Genome Res.* **10**, 1890-1902.

Prince, V. E. (2002). The hox paradox: more complex(es) than imagined. *Dev. Biol.* **249**, 1-15.

Prince, V. E., Joly, L., Ekker, M. and Ho, R. K. (1998). Zebrafish hox genes: genomic organization and modified colinear expression patterns in the trunk. *Development* **125**, 407-420.

Reifers, F., Bohli, H., Walsh, E. C., Crossley, P. H., Stainier, D. Y. and Brand, M. (1998). Fgf8 is mutated in zebrafish *acerebellar (ace)* mutants and is required for maintenance of midbrain-hindbrain boundary development and somitogenesis. *Development* **125**, 2381-2395.

Reifers, F., Adams, J., Mason, I. J., Schulte-Merker, S. and Brand, M. (2000). Overlapping and distinct functions provided by fgf17, a new zebrafish member of the Fgf8/17/18 subgroup of Fgfs. *Mech. Dev.* **99**, 39-49.

Schulte-Merker, S., Ho, R. K., Herrmann, B. G. and Nusslein-Volhard, C. (1992). The protein product of the zebrafish homologue of the mouse *T* gene is expressed in nuclei of the germ ring and the notochord of the early embryo. *Development* **116**, 1021-1032.

Schulte-Merker, S., van Eeden, F. J., Halpern, M. E., Kimmel, C. B. and Nusslein-Volhard, C. (1994). *no tail (ntl)* is the zebrafish homologue of the mouse *T (Brachyury)* gene. *Development* **120**, 1009-1015.

Schulte-Merker, S. and Smith, J. C. (1995). Mesoderm formation in response to Brachyury requires FGF signalling. *Curr. Biol*. **5**, 62-67.

Sekine, K., Ohuchi, H., Fujiwara, M., Yamasaki, M., Yoshizawa, T., Sato, T., Yagishita, N., Matsui, D., Koga, Y., Itoh, N. and Kato, S. (1999). Fgf10 is essential for limb and lung formation. *Nat. Genet.* **21**, 138-141.

Smith, J. (1999). T-box genes: what they do and how they do it. *Trends Genet.* **15**, 154-158.

Smith, J. C., Price, B. M. J., Green, J. B. A., Weigel, D. and Herrmann, B. G. (1991). Expression of a *Xenopus* homolog of *Brachyury* (T) is an immediate-early response to mesoderm induction. *Cell* **67**, 79-87.

Stennard, F., Carnac, G., and Gurdon, J. B. (1996). The *Xenopus* T-box gene, *Antipodean*, encodes a vegetally localised maternal mRNA and can trigger mesoderm formation. *Development* **122**, 4179-4188.

Sun, X., Meyers, E. N., Lewandoski, M. and Martin, G. R. (1999). Targeted disruption of Fgf8 causes failure of cell migration in the gastrulating mouse embryo. *Genes Dev.* **13**, 1834-1846.

Ueno, H., Gunn, M., Dell, K., Tseng, A. and Williams, L. T. (1992). A truncated form of fibroblast growth factor receptor 1 inhibits signal transduction by multiple types of fibroblast growth factor receptors. *J. Biol. Chem.* **267**, 1470-1476.

Vitelli, F., Taddei, I., Morishima, M., Meyers, E. N., Lindsay, E. A. and Baldini, A. (2002). A genetic link between Tbx1 and fibroblast growth factor signaling. *Development* **129**, 4605-4611.

Wall, N. A. and Hogan, B. L. M. (1995). Expression of bone morphogenetic protein-4 (BMP-4), bone morphogenetic protein 7 (BMP-7), fibroblast growth factor-8 (FGF-8) and sonic hedgehog (SHH) during branchial arch development in the chick. *Mech. Dev.* **53**, 383-392.

Warga, R. M. and Kimmel, C. B. (1990). Cell movements during epiboly and gastrulation in zebrafish. *Development* **108**, 569-580.

Warga, R. M. and Nusslein-Volhard, C. (1999). Origin and development of the zebrafish endoderm. *Development* **126**, 827-838.

Weinberg, E. S., Allende, M. L., Kelly, C. S., Abdelhamid, A., Murakami, T., Andermann, P., Doerre, O. G., Grunwald, D. J. and Riggleman, B. (1996). Developmental regulation of zebrafish MyoD in wild-type, *no tail* and *spadetail* embryos. *Development* **122**, 271-280.

Westerfield, M. (1995). *The Zebrafish Book*. University of Oregon; Eugene, OR.

Whitlock, K. E. and Westerfield, M. (2000). The olfactory placodes of the zebrafish form by convergence of cellular fields at the edge of the neural plate. *Development* **127**, 3645-3653.

Whitmore, T. E., Maurer, M. F., Sexson, S., Raymond, F., Conklin, D. and Deisher, T. A. (2000). Assignment of fibroblast growth factor 18 (FGF18) to human chromosome 5q34 by use of radiation hybrid mapping and fluorescence in situ hybridization. *Cytogenet Cell Genet.* **90**, 231-233.

Wilkinson, D. G., Peters, G., Dickson, C. and McMahon, A. (1988). Expression of the FGF-related proto-oncogene *int-2* during gastrulation ans neurulation in the mouse. *EMBO J.* **7**, 691-695.

Woods, I. G., Kelly, P. D., Chu, F., Ngo-Hazelett, P., Yan, Y.-L., Huang, H., Postlethwait, J. H. and Talbot, W. S. (2000). A comparative map of the zebrafish genome. *Genome Res.* **10**, 1903-1914.

Xu, J., Liu, Z. and Ornitz, D. M. (2000). Temporal and spatial gradient of *Fgf8* and *Fgf17* regulate proliferation and differentiation of midline cerebellar structures. *Development* **127**, 1833-1843.

Xu, X., Weinstein, M., Li, C., Naski, M., Cohen, R. I., Ornitz, D. M., Leder, P. and Deng, C. (1998). Fibroblast growth factor receptor 2 (FGFR2)-mediated reciprocal regulation loop between FGF8 and FGF10 is essential for limb induction. *Development* **125**, 753-765.

Yamaguchi, T. P., Harpal, K., Henkemeyer, M. and Rossant, J. (1994). *fgfr-1* is required for embryonic growth and mesodermal patterning during mouse gastrulation. *Genes Dev.* **8**, 3032-3044.

Zhang, J. and King, M. L. (1996). *Xenopus VegT* RNA is localized to the vegetal cortex during oogenesis and encodes a novel T-box transcription factor involved in mesodermal patterning. *Development* **122**, 4119-4129.

Zhang, J., Houston, D. W., King, M. L., Payne, C., Wylie, C. and Heasman, J. (1998). The role of maternal VegT in establishing the primary germ layers in *Xenopus* embryos. *Cell* **94**, 515-524.